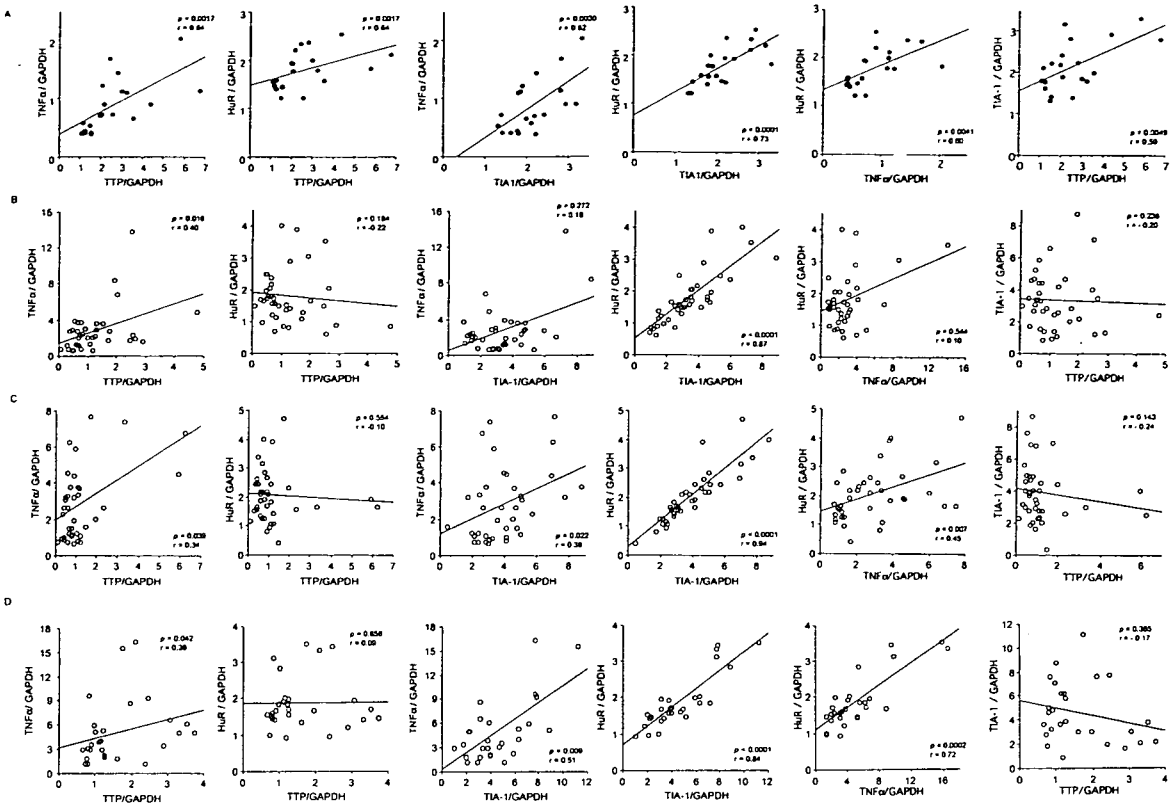

Figure 3. Relationships between expression levels of tumor necrosis factor α (TNFα) and adenine/uridine-rich element binding protein genes in peripheral blood mononuclear cells obtained from patients with rheumatoid arthritis (RA; open circles [n = 38]) and from healthy control subjects (solid circles [n = 20]). **A**, Healthy control subjects. **B**, Patients with RA, before initiation of infliximab therapy. **C**, Patients with RA, 2 weeks after administration of the first dose of infliximab. **D**, Patients with RA, 54 weeks after initiation of infliximab therapy. *P* values were calculated using Pearson's correlation coefficient. See Figure 1 for other definitions.

achieve at least an ACR20 response at week 54 were included in the nonresponder group. No significant differences in the expression of TNFα and ABP genes were observed between these 2 groups (for TNFα, 3.27 ± 3.53 in responders and 2.18 ± 1.25 in nonresponders; for TTP, 1.20 ± 1.31 in responders and 1.09 ± 0.50 in nonresponders; for TIA-1, 3.55 ± 1.64 in responders and 2.86 ± 1.01 in responders; for HuR, 1.72 ± 0.68 in responders and 1.86 ± 0.92 in nonresponders) (Figure 4). The TIA-1:HuR gene expression ratio at week 0 tended to be higher in the responder group than in the nonresponder group (2.051 ± 0.471 and 1.626 ± 0.365, respectively [P = 0.059 by Mann-Whitney U test]). No statistically significant differences were observed between responders and nonresponders for other clinical parameters measured at week 0 or week 2, including serum CRP levels, the erythrocyte sedimentation rate, and other ACR-defined improvement parameters, and the matrix metalloproteinase 3 level (data not shown).

DISCUSSION

In this study, we investigated the role of ABPs in the pathogenesis of RA, as well as any association between gene expression and the efficacy of anti-TNFα therapy, by monitoring PBMC samples obtained before and after infliximab therapy. A similar study using synovial tissue would have been preferable but is quite impractical. We anticipated that the gene expression levels of TNFα and the ABPs in PBMCs would reflect the inflammation status of patients with RA, and we focused on TTP, TIA-1, and HuR, which are clinically important ABPs. Results of previous studies suggested that TTP and TIA-1 are antiinflammatory factors, while HuR is considered an inflammation-accelerating factor

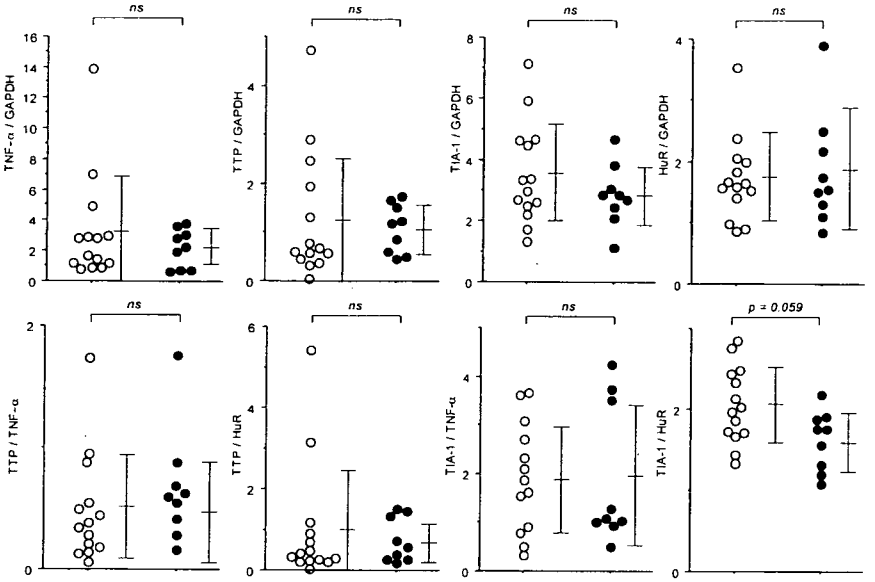

Figure 4. Relationships between expression levels of TNFα and adenine/uridine-rich element binding protein genes in peripheral blood mononuclear cells, and efficacy of infliximab therapy. Open circles represent the 14 rheumatoid arthritis patients who achieved 50% improvement according to the American College of Rheumatology response criteria (ACR50) at week 54. Solid circles represent the 9 patients who had not achieved at least an ACR20 response at week 54. Bars show the mean ± SD. *P* values were calculated by Mann-Whitney U test. NS = not significant (see Figure 1 for other definitions).

(28,33,34,36,39,41,42). We speculated that the balance or imbalance in the production of these factors may induce differences in TNFα production, and hence, RA activity.

The aim of anti-TNFα therapy is to neutralize TNFα in the circulation and suppress the harmful effects of this cytokine in vivo. In doing so, the physiologic mechanisms that control TNFα gene transcription may be attenuated in the short term, resulting in increased TNFα production. If this is the case, differences in the posttranscriptional regulation of TNFα production may affect the disease activity or efficacy of TNFα-blocking agents in individual patients with RA. Therefore, examining the gene expression of TNFα and ABP may provide not only a better understanding of the pathogenesis of RA but also a clue to the factors that affect and allow us to predict the efficacy of TNFα-blocking drugs.

Our results showed that prior to the start of infliximab therapy, the TNFα gene was overexpressed and the TTP gene was underexpressed in patients with RA compared with healthy control subjects. Furthermore, the TTP:TNFα and TTP:HuR ratios were significantly lower in patients with RA than in healthy control subjects. Because TTP is a destabilizer of TNFα mRNA, and various stimuli including TNFα itself promote TTP production (33), our results imply that the negative feedback mechanism of TTP production is not sufficient to counter the excessive TNFα production that occurs during active RA. TIA-1 gene expression and the TIA-1:HuR expression ratio were higher in patients with RA than in control subjects, while the TIA-1:TNFα ratio was lower. Because TIA-1 is a translational silencer of TNFα, it is conceivable that TIA-1 is produced as another negative feedback mechanism against TNFα overproduction to compensate for the TTP decrement in patients with active RA, although such compensation is still not sufficient to mitigate the symptoms of RA activity. Interestingly, although the scatter in expression of the TIA-1 gene was small among healthy control subjects, it was quite large among patients with RA. This may reflect the interindividual differences in the regulation of TIA-1 expression, which become evident when a person acquires an inflammatory disorder mediated by TNFα.

Considering the crucial role of excessive TNFα production in the RA inflammatory process, abnormal regulation at the posttranscriptional level may be one of the factors that promote this excessive TNFα production, and thus, more severe arthritis. We previously reported that TTP gene expression is significantly higher in RA synovial tissue compared with that in OA synovial

tissue (40). One of the explanations for this discrepancy is that in the previous study, RA synovial samples were obtained from patients who had undergone surgery, and disease activity greatly varied among these patients. In contrast, all of the PBMC samples used in the present study were obtained from patients with active arthritis and were obtained just prior to initiation of anti-TNFα therapy. Another interpretation is that TTP production may be higher at sites of active inflammation (e.g., synovial tissue in patients with RA) than in PBMCs.

To investigate the effect of infliximab on the production of TNFα posttranscriptional regulatory factors, we compared the gene expression levels of TNFα and the 3 ABPs before and 2 weeks and 54 weeks after administration of the first dose of infliximab. There were no significant changes in gene expression, but the TTP:HuR ratio significantly decreased after infliximab therapy. This change may have resulted from the decrease in TTP gene expression and the increase in HuR gene expression in response to infliximab-induced TNFα removal. The results hinted at this situation but were not statistically significant. In addition, the TIA-1:TNFα ratio tended to increase at week 2. This may also have resulted from a subtle reduction in TNFα gene expression and an increase in TIA-1 gene expression. When gene expression at week 0 and week 54 were compared, TNFα gene expression and the TIA-1:HuR ratio were significantly higher in week 54 samples than in week 0 samples. Inhibition of the function of the TNFα protein by infliximab may have led to a relative increment in expression of the TNFα gene and the TIA-1 gene.

Interestingly, parameters investigated in this study tended to fluctuate toward the reverse direction when changes between week 0 and week 2 and those between week 2 and week 54 were compared. In addition, there seemed to be a large interindividual difference in the fluctuation of these parameters, especially TTP, TIA-1, HuR, the TIA-1:TNFα ratio, and the TIA-1:HuR ratio. These results imply that the impact of infliximab on the posttranscriptional regulation of TNFα production varies among individual patients with RA. These variations may affect the long-term efficacy of anti-TNFα drugs. Recently, it has been discussed whether infliximab therapy could be postponed in some patients without causing a flare in disease activity (45). Gene expression levels of TNFα and ABPs that are involved in the posttranscriptional regulation of TNFα production are possible candidates for parameters that could be used to predict whether infliximab may be withdrawn without a severe flare in disease activity.

A significant positive relationship was observed between the gene expression of TNFα and that of TTP, in PBMC samples from both patients with RA and healthy control subjects. This result is consistent with results of a previous study showing induction of TTP protein biosynthesis by TNFα production in macrophages as a part of a negative feedback mechanism (33). The correlation between TNFα and TTP was most prominent in healthy subjects, which may imply that the balance of TNFα and TTP gene expression is inappropriately regulated in at least some patients with RA. The positive relationship of TNFα and TIA-1, in both patients with RA and healthy control subjects, implies that a negative feedback mechanism between TNFα and TIA-1 may also exist. In addition, a strong positive relationship was observed between the gene expression of TIA-1 and that of HuR in both patients with RA and healthy control subjects, implying that either a common mechanism controlling the expression of TIA-1 and HuR is present or that one of these proteins controls the expression of the other. Interestingly, we also observed a strong positive relationship between the expression of TIA-1 and that of HuR genes in synovial tissue obtained from patients with RA after surgery (46).

Recently, it was shown in HuR-transgenic mice that HuR and TIA-1 act in concert to suppress TNFα production, suggesting that HuR may be an inflammation suppressor in vivo (26), contrary to previous studies in which HuR was reported to be a proinflammatory factor (39,41,42). Thus, it seems that ABPs do not function independently of each other, and the precise roles of these ABPs in vivo are still to be elucidated. In contrast to what is observed in healthy control subjects, positive correlations between TTP and HuR gene expression and between TTP and TIA-1 were not present in RA samples obtained before and 2 weeks after initiation of infliximab therapy. It is possible that an imbalance in gene expression is one of the causes of excessive TNFα production, which in turn leads to higher disease activity in patients with RA.

Currently, it is not clear why the efficacy of TNFα-blocking agents differs greatly among patients with RA. We wanted to find some clues that may help answer this question. The TIA-1:HuR gene expression ratio tended to be higher in the responder group, but the difference between responders and nonresponders was not statistically significant. It may be possible that patients with lower gene expression of HuR and higher expression of TIA-1 have decreased TNFα mRNA stability and translation, and hence, lower TNFα production. In these patients, infliximab might be more effective in neutralizing circulating TNFα than in patients

with a lower TIA-1:HuR expression ratio. Measurement of such gene expression in patients prior to infliximab therapy might be a useful predictor of the potential efficacy of infliximab. However, we were unable to draw a definitive conclusion in this study, and additional studies with a larger number of samples should be performed to confirm our observations and speculations. In a recent study, it was shown that failure to suppress serum CRP at week 2 of therapy identified the majority of patients who were nonresponders by week 12 (47). However, in our series of patients, we did not find a significant relationship between a reduction in the CRP level at week 2 and the efficacy of infliximab at week 54.

Our study had several limitations. Although we included all of our patients who were receiving infliximab therapy, the cohort number was not large enough for strong statistical analyses. Protein analyses would also be useful to accurately determine the ABP levels actually present in the cells. Other ABPs that were not studied here may also have important roles in the pathogenesis of RA. Furthermore, the ABPs studied here can also affect the mRNA of other inflammatory molecules such as cyclooxygenase 2 (48–50); these interactions may have impacted our findings and therefore should be considered in any interpretation of the data.

In conclusion, by analyzing the gene expression levels of TNFα and ABP in PBMCs, we observed a relationship between the expression of TTP, TIA-1, and HuR that might have an impact on TNFα gene expression and thereby protein production. Our results also implied that the TIA-1:HuR gene expression ratio before infliximab therapy may predict the efficacy of treatment. Further studies are necessary to enhance our understanding of RA pathogenesis and to identify possible targets of therapy as well as parameters that predict the efficacy of pharmaceutical agents.

ACKNOWLEDGMENTS

We thank Takanori Yasukochi for the helpful discussion, and Hiromi Yuhashi and Yoko Kitamura for the excellent technical support.

AUTHOR CONTRIBUTIONS

Dr. Sumida had full access to all of the data in the study and takes responsibility for the integrity of the data and the accuracy of the data analysis.

Study design. Sugihara, Tsutsumi, E. Suzuki, Sumida.

Acquisition of data. Sugihara, Tsutsumi, E. Suzuki, T. Suzuki, Ogishima, Hayashi, Chino, Ishii, Mamura, Goto, Matsumoto, Ito, Sumida.

Analysis and interpretation of data. Sugihara, Tsutsumi, Wakamatsu, Sumida.

Manuscript preparation. Sugihara, Tsutsumi, Sumida.

Statistical analysis. Sugihara, Tsutsumi, Sumida.

REFERENCES

1. Spector TD. Rheumatoid arthritis [review]. Rheum Dis Clin North Am 1990;16:513–37.
2. Saxne T, Palladino MA Jr, Heinegard D, Talal N, Wollheim FA. Detection of tumor necrosis factor α but not tumor necrosis factor β in rheumatoid arthritis synovial fluid and serum. Arthritis Rheum 1988;31:1041–5.
3. Hopkins SJ, Meager A. Cytokines in synovial fluid. II. The presence of tumour necrosis factor and interferon. Clin Exp Immunol 1988;73:88–92.
4. Tetta C, Camussi G, Modena V, Di Vittorio C, Baglioni C. Tumour necrosis factor in serum and synovial fluid of patients with active and severe rheumatoid arthritis. Ann Rheum Dis 1990;49:665–7.
5. Rannou F, Francois M, Corvol MT, Berenbaum F. Cartilage breakdown in rheumatoid arthritis [review]. Joint Bone Spine 2006;73:29–36.
6. Kay J, Calabrese L. The role of interleukin-1 in the pathogenesis of rheumatoid arthritis. Rheumatology (Oxford) 2004;43 Suppl 3:iii2–9.
7. Nishimoto N. Interleukin-6 in rheumatoid arthritis. Curr Opin Rheumatol 2006;18:277–81.
8. Zhang HG, Hyde K, Page GP, Brand JP, Zhou J, Yu S, et al. Novel tumor necrosis factor α–regulated genes in rheumatoid arthritis. Arthritis Rheum 2004;50:420–31.
9. Keystone EC, Schiff MH, Kremer JM, Kafka S, Lovy M, DeVries T, et al. Once-weekly administration of 50 mg etanercept in patients with active rheumatoid arthritis: results of a multicenter, randomized, double-blind, placebo-controlled trial. Arthritis Rheum 2004;50:353–63.
10. Maini RN, Breedveld FC, Kalden JR, Smolen JS, Davis D, Macfarlane JD, et al. Therapeutic efficacy of multiple intravenous infusions of anti–tumor necrosis factor α monoclonal antibody combined with low-dose weekly methotrexate in rheumatoid arthritis. Arthritis Rheum 1998;41:1552–63.
11. Elliott MJ, Maini RN, Feldmann M, Kalden JR, Antoni C, Smolen JS, et al. Randomised double-blind comparison of chimeric monoclonal antibody to tumour necrosis factor α (cA2) versus placebo in rheumatoid arthritis. Lancet 1994;344:1105–10.
12. Maini R, St.Clair EW, Breedveld F, Furst D, Kalden J, Weisman M, et al, for the ATTRACT Study Group. Infliximab (chimeric anti-tumour necrosis factor α monoclonal antibody) versus placebo in rheumatoid arthritis patients receiving concomitant methotrexate: a randomised phase III trial. Lancet 1999;354:1932–9.
13. Kavanaugh A, St.Clair EW, McCune WJ, Braakman T, Lipsky P. Chimeric anti-tumor necrosis factor-α monoclonal antibody treatment of patients with rheumatoid arthritis receiving methotrexate therapy. J Rheumatol 2000;27:841–50.
14. Lipsky PE, van der Heijde DM, St.Clair EW, Furst DE, Breedveld FC, Kalden JR, et al, for the Anti-Tumor Necrosis Factor Trial in Rheumatoid Arthritis with Concomitant Therapy Study Group. Infliximab and methotrexate in the treatment of rheumatoid arthritis. N Engl J Med 2000;343:1594–602.
15. Moreland LW, Schiff MH, Baumgartner SW, Tindall EA, Fleischmann RM, Bulpitt KJ, et al. Etanercept therapy in rheumatoid arthritis: a randomized, controlled trial. Ann Intern Med 1999;130:478–86.
16. Weinblatt ME, Kremer JM, Bankhurst AD, Bulpitt KJ, Fleischmann RM, Fox RI, et al. A trial of etanercept, a recombinant tumor necrosis factor receptor:Fc fusion protein, in patients with rheumatoid arthritis receiving methotrexate. N Engl J Med 1999;340:253–9.
17. Klareskog L, van der Heijde D, de Jager JP, Gough A, Kalden J, Malaise M, et al. Therapeutic effect of the combination of etanercept and methotrexate compared with each treatment alone in patients with rheumatoid arthritis: double-blind randomised controlled trial. Lancet 2004;363:675–81.
18. Den Broeder A, van de Putte L, Rau R, Schattenkirchner M, Van Riel P, Sander O, et al. A single dose, placebo controlled study of

the fully human anti-tumor necrosis factor-α antibody adalimumab (D2E7) in patients with rheumatoid arthritis. J Rheumatol 2002; 29:2288–98.
19. Weinblatt ME, Keystone EC, Furst DE, Moreland LW, Weisman MH, Birbara CA, et al. Adalimumab, a fully human anti–tumor necrosis factor α monoclonal antibody, for the treatment of rheumatoid arthritis in patients taking concomitant methotrexate: the ARMADA trial. Arthritis Rheum 2003;48:35–45.
20. Breedveld FC, Weisman MH, Kavanaugh AF, Cohen SB, Pavelka K, van Vollenhoven R, et al. The PREMIER study: a multicenter, randomized, double-blind clinical trial of combination therapy with adalimumab plus methotrexate versus methotrexate alone or adalimumab alone in patients with early, aggressive rheumatoid arthritis who had not had previous methotrexate treatment. Arthritis Rheum 2006;54:26–37.
21. Nishimoto N, Yoshizaki K, Miyasaka N, Yamamoto K, Kawai S, Takeuchi T, et al. Treatment of rheumatoid arthritis with humanized anti–interleukin-6 receptor antibody: a multicenter, double-blind, placebo-controlled trial. Arthritis Rheum 2004;50:1761–9.
22. Chen CY, Shyu AB. AU-rich elements: characterization and importance in mRNA degradation. Trends Biochem Sci 1995;20:465–70.
23. Ross J. mRNA stability in mammalian cells. Microbiol Rev 1995;59:423–50.
24. Jacobson A, Peltz SW. Interrelationships of the pathways of mRNA decay and translation in eukaryotic cells [review]. Annu Rev Biochem 1996;65:693–739.
25. Dean JL, Sully G, Clark AR, Saklatvala J. The involvement of AU-rich element-binding proteins in p38 mitogen-activated protein kinase pathway-mediated mRNA stabilisation. Cell Signal 2004;16:1113–21.
26. Katsanou V, Papadaki O, Milatos S, Blackshear PJ, Anderson P, Kollias G, et al. HuR as a negative posttranscriptional modulator in inflammation. Mol Cell 2005;19:777–89.
27. Ma WJ, Cheng S, Campbell C, Wright A, Furneaux H. Cloning and characterization of HuR, a ubiquitously expressed Elav-like protein. J Biol Chem 1996;271:8144–51.
28. Piecyk M, Wax S, Beck AR, Kedersha N, Gupta M, Maritim B, et al. TIA-1 is a translational silencer that selectively regulates the expression of TNF-α. EMBO J 2000;19:4154–63.
29. DuBois RN, McLane MW, Ryder K, Lau LF, Nathans D. A growth factor-inducible nuclear protein with a novel cysteine/histidine repetitive sequence. J Biol Chem 1990;265:19185–91.
30. Lai WS, Stumpo DJ, Blackshear PJ. Rapid insulin-stimulated accumulation of an mRNA encoding a proline-rich protein. J Biol Chem 1990;265:16556–63.
31. Ma Q, Herschman HR. A corrected sequence for the predicted protein from the mitogen-inducible TIS11 primary response gene. Oncogene 1991;6:1277–8.
32. Varnum BC, Lim RW, Sukhatme VP, Herschman HR. Nucleotide sequence of a cDNA encoding TIS11, a message induced in Swiss 3T3 cells by the tumor promoter tetradecanoyl phorbol acetate. Oncogene 1989;4:119–20.
33. Carballo E, Lai WS, Blackshear PJ. Feedback inhibition of macrophage tumor necrosis factor-α production by tristetraprolin. Science 1998;281:1001–5.
34. Carballo E, Gilkeson GS, Blackshear PJ. Bone marrow transplantation reproduces the tristetraprolin-deficiency syndrome in recombination activating gene-2 (−/−) mice: evidence that monocyte/macrophage progenitors may be responsible for TNFα overproduction. J Clin Invest 1997;100:986–95.
35. Dember LM, Kim ND, Liu KQ, Anderson P. Individual RNA recognition motifs of TIA-1 and TIAR have different RNA binding specificities. J Biol Chem 1996;271:2783–8.
36. Phillips K, Kedersha N, Shen L, Blackshear PJ, Anderson P. Arthritis suppressor genes TIA-1 and TTP dampen the expression of tumor necrosis factor α, cyclooxygenase 2, and inflammatory arthritis. Proc Natl Acad Sci U S A 2004;101:2011–6.
37. Fan XC, Steitz JA. Overexpression of HuR, a nuclear-cytoplasmic shuttling protein, increases the in vivo stability of ARE-containing mRNAs. EMBO J 1998;17:3448–60.
38. Peng SS, Chen CY, Xu N, Shyu AB. RNA stabilization by the AU-rich element binding protein, HuR, an ELAV protein. EMBO J 1998;17:3461–70.
39. Dean JL, Wait R, Mahtani KR, Sully G, Clark AR, Saklatvala J. The 3′ untranslated region of tumor necrosis factor α mRNA is a target of the mRNA-stabilizing factor HuR. Mol Cell Biol 2001; 21:721–30.
40. Tsutsumi A, Suzuki E, Adachi Y, Murata H, Goto D, Kojo S, et al. Expression of tristetraprolin (G0S24) mRNA, a regulator of tumor necrosis factor-α production, in synovial tissues of patients with rheumatoid arthritis. J Rheumatol 2004;31:1044–9.
41. Di Marco S, Hel Z, Lachance C, Furneaux H, Radzioch D. Polymorphism in the 3′-untranslated region of TNFα mRNA impairs binding of the post-transcriptional regulatory protein HuR to TNFα mRNA. Nucleic Acids Res 2001;29:863–71.
42. McMullen MR, Cocuzzi E, Hatzoglou M, Nagy LE. Chronic ethanol exposure increases the binding of HuR to the TNFα 3′-untranslated region in macrophages. J Biol Chem 2003;278: 38333–41.
43. Arnett FC, Edworthy SM, Bloch DA, McShane DJ, Fries JF, Cooper NS, et al. The American Rheumatism Association 1987 revised criteria for the classification of rheumatoid arthritis. Arthritis Rheum 1988;31:315–24.
44. Felson DT, Anderson JJ, Boers M, Bombardier C, Furst D, Goldsmith C, et al. American College of Rheumatology preliminary definition of improvement in rheumatoid arthritis. Arthritis Rheum 1995;38:727–35.
45. Allaart CF, Goekoop-Ruiterman YP, de Vries-Bouwstra JK, Breedveld FC, Dijkmans BA, Group FS. Aiming at low disease activity in rheumatoid arthritis with initial combination therapy or initial monotherapy strategies: the BeSt study. Clin Exp Rheumatol 2006;24(6 Suppl 43):S077–82.
46. Suzuki E, Tsutsumi A, Sugihara M, Mamura M, Goto D, Matsumoto I, et al. Expression of TNF-α, tristetraprolin, T-cell intracellular antigen-1 and Hu antigen R genes in synovium of patients with rheumatoid arthritis. Int J Mol Med 2006;18:273–8.
47. Buch MH, Seto Y, Bingham SJ, Bejarano V, Bryer D, White J, et al. C-reactive protein as a predictor of infliximab treatment outcome in patients with rheumatoid arthritis: defining subtypes of nonresponse and subsequent response to etanercept. Arthritis Rheum 2005;52:42–8.
48. Sully G, Dean JL, Wait R, Rawlinson L, Santalucia T, Saklatvala J, et al. Structural and functional dissection of a conserved destabilizing element of cyclo-oxygenase-2 mRNA: evidence against the involvement of AUF-1 [AU-rich element/poly(U)-binding/degradation factor-1], AUF-2, tristetraprolin, HuR (Hu antigen R) or FBP1 (far-upstream-sequence-element-binding protein 1). Biochem J 2004;377:629–39.
49. Cok SJ, Acton SJ, Morrison AR. The proximal region of the 3′-untranslated region of cyclooxygenase-2 is recognized by a multimeric protein complex containing HuR, TIA-1, TIAR, and the heterogeneous nuclear ribonucleoprotein U. J Biol Chem 2003;278:36157–62.
50. Dixon DA, Balch GC, Kedersha N, Anderson P, Zimmerman GA, Beauchamp RD, et al. Regulation of cyclooxygenase-2 expression by the translational silencer TIA-1. J Exp Med 2003;198:475–81.

parental genetic testing identified an identical nucleotide missense substitution in the mother, but not in the father.

Improved clinical symptoms after inhibition of interleukin 1 (IL 1) activity by anakinra was reported in all of the cryopyrin-associated autoinflammatory syndromes, although treatment failure has also been reported.[1–4] Therapy with IL 1 antagonism was begun in our patient at 9 years and a clinical response was reported within days. On taking Anakinra (~0.90 mg/kg/day) his energy level improved, his rash appeared less frequently and his arthritis and conjunctivitis were resolved. His erythrocyte sedimentation rate, white cell count and platelet count all improved (table 1). The patient's family temporarily reduced the dose of anankinra to 0.30 mg/kg/day, and he again experienced clinical and laboratory evidence of disease flare, indicating a dose-dependent response (table 1).

In all, 60 different dominantly inherited missense mutations within exon three of CIAS1 have been associated with the three heterogeneous cryopyrin-associated autoinflammatory syndromes.[5 6] Previous patients described with characteristics of both familial cold-induced autoinflammatory syndrome and Muckle–Wells syndrome have had other unique cryopyrin mutations that were distinct from the new mutation described here.[1 7] It is interesting to note that two other mutations that would cause different amino acid substitutions at this site (Thr436iie; Thr436Asn) were reported in patients with chronic infantile neurological cutaneous articular syndrome. [8] These findings would suggest that specific amino acid substitutions at this site are solely responsible for the clinical phenotype. However, phenotypic heterogeneity, including incomplete penetrance among family members, has been described among individuals carrying identical mutations.[7 9 10] Thus there is probably an effect of additional modifier genes or environmental factors in the phenotypic expression of the cryopyrin-associated autoinflammatory syndromes.[8]

ACKNOWLEDGEMENTS

Helpful input and comments from Dr John Carey are appreciated.

Authors' affiliations

Andrew Zeft, John F Bohnsack, Division of Immunology and Rheumatology, Department of Pediatrics, University of Utah, Salt Lake City, Utah, USA

Competing interests: None.

Correspondence to: Dr A Zeft, Division of Immunology and Rheumatology, Department of Pediatrics University of Utah, 30 North 1900 East, #2A134 SOM, Salt Lake City, UT 84132, USA; andrew.zeft@hsc.utah.edu

Accepted 18 February 2007

REFERENCES

1 Hawkins PNLH, Aganna E, McDermott MF. Spectrum of clinical features in Muckle–Wells syndrome and response to anakinra. *Arthritis and Rheumatism* 2004;50:607–12.
2 Hoffman HMRS, Boyle DL, Cho JY, Nayar J, Mueller JL, Anderson JP, *et al.* Prevention of cold-associated acute inflammation in familial cold autoinflammatory syndrome by interleukin-1 receptor antagonist. *Lancet* 2004;364:1779–85.
3 Goldbach-Mansky RDN, Canna SW, Gelabert A, Jones J, Rubin BI, Kim HJ, *et al.* Neonatal-onset multisystem inflammatory disease responsive to interleukin-1beta inhibition. *New Engl J Med* 2006;355:581–92.
4 Matsubara THM, Shiraishi M, Hoffman HM, Ichiyama T, Tanaka T, Ueda H, *et al.* A severe case of chronic infantile neurologic, cutaneous, articular syndrome treated with biologic agents. *Arthritis Rheum* 2006;54:2314–20.
5 Touitou ILS, McDermott M, Cuisset L, Hoffman H, Dode C, Shoham N, Aganna E, *et al.* Infevers: an evolving mutation database for auto-inflammatory syndromes. *Hum Mutat* 2004;24:194–8.
6 Touitou I. INFEVERS Web site. 2002. http://fmf/igh.cnrs.fr/infevers/ (accessed 12 March 2007).
7 Dode CLDN, Cuisset L, Letourneur F, Berthelot JM, Vaudour G, Meyrier A, *et al.* New mutations of CIAS1 that are responsible for Muckle–Wells syndrome and familial cold urticaria: a novel mutation underlies both syndromes. *Am J Hum Genet* 2002;70:1498–506.
8 Hull KMSN, Chae JJ, Aksentijevich I, Kastner DL. The expanding spectrum of systemic autoinflammatory disorders and their rheumatic manifestations. *Curr Opin Rheumatol* 2003;15:61–9.
9 Arostegui JIAA, Modesto C, Rua MJ, Arguelles F, Gonzalez-Ensenat MA, Ramos E, *et al.* Clinical and genetic heterogeneity among Spanish patients with recurrent autoinflammatory syndromes associated with the CIAS1/PYPAF1/NALP3 gene. *Arthritis Rheum* 2004;50:4045–50.
10 Hoffman HMMJ, Broide DH, Wanderer AA, Kolodner RD. Mutation of a new gene encoding a putative pyrin-like protein causes familial cold autoinflammatory syndrome and Muckle–Wells syndrome. *Nat Genet* 2001;29:301–5.

DNA microarray analysis of labial salivary glands of patients with Sjögren's syndrome

Ei Wakamatsu, Yumi Nakamura, Isao Matsumoto, Daisuke Goto, Satoshi Ito, Akito Tsutsumi, Takayuki Sumida

Ann Rheum Dis 2007;66:844–845. doi: 10.1136/ard.2006.063370

Sjögren's syndrome (SS) is a chronic autoimmune disease characterised by dry eyes, dry mouth and focal lymphocytic infiltration in lacrimal and salivary glands. The infiltrating lymphocytes are mainly CD4 α/β T cells,[1] especially T helper 1 (Th1) type T cells, because they produce both interferon (IFN)γ and interleukin 2.[2 3] To understand the pathogenesis of SS, several molecules in labial salivary glands (LSGs) have been screened by microarray analysis in human SS. Hjelmervik *et al*[4] and Gottenberg *et al*[5] reported that the upregulated genes in SS salivary glands were IFN-inducible genes, such as IFN-stimulated transcription factor 3, IFN-regulatory factor 1 and B cell-activation factor of the TNF family. However, there is little or no information on the essential genes involved in the generation of sialoadenitis in patients with SS. We screened abnormally expressed genes in LSGs of patients with SS using cDNA microarray technology to elucidate the SS susceptibility genes.

The cDNA array was performed using total RNA from LSGs of three patients with primary SS and from three healthy subjects (control) with a DNA chip including 775 genes (JGS, Tokyo, Japan). The DNA chip contained immunoglobulins, human leucocyte antigens (HLAs), complements, T cell receptors (TCRs), IFN-inducible proteins, cytokines, transcriptional factors and other autoimmune disease-related genes. Abnormally

Abbreviations: HLA, human leucocyte antigen; SS, Sjögren's syndrome; IFN, interferon; LSG, labial salivary gland Th1, T helper cell; TCR, T cell receptor

Table 1 Genes expressed in labial salivary glands of patients with Sjögren's syndrome (SS)

Gene name	SS/HS
Upregulated genes	
Immunoglobulin (Ig)	
Ig heavy constant γ3	8.40*
Igγ chain, Ig rearranged γ chain, V-J-C region	2.99*
Ig κ variable 1D8	3.25*
Rearranged Ig mRNA for μ heavy chain enhancer and constant region	2.23*
Human leucocyte antigen (HLA)	
Human MHC HLA class I cell surface antigen (HLA-B 5102) mRNA	6.56*
HLA-F	3.31*
HLA-DRβ1	6.22*
HLA-DP light chain	3.01*
RING6 (HLA class II α chain-like product)	2.41*
MHC class II DQ	2.35*
MHC class II DR	7.28*
Complement	
Complement C3	3.96*
T cell receptor (TCR)	
TCRβ chain (T cell receptor β chain)	2.11*
Interferon (IFN)-inducible genes	
IP-30 (IFNγ-inducible protein)	2.17*
I-5 I.1 (IFNγ-inducible gene)	2.25*
IP-10 (IFNγ-inducible chemokine)	2.31*
IFNα/β-inducible p44	2.1*
IFN-α-inducible protein 27	2.19*
Stat50 mRNA	2.04*
Thymosin β	
Thymosin β4	2.03*
Thymosin β10	2.12*
Transcription factor	
STAT1α	2.88*
STAT1β	2.07*
I κ Bβ	2.02*
Downregulated genes	
LIM protein (cystein-rich protein 3)	0.44*

MHC, major histocompatibility complex.
The average of patients with SS, healthy subjects based on cDNA array fluorescent data (healthy subjects (n = 3, each). The Mann–Whitney U test was used to compare the control and SS groups.
*p<0.05.

expressed genes in SS LSG represented those with expression level over twofold or below 0.5-fold of that of LSGs of the controls. The Mann–Whitney U test was used for statistical analysis. p Values <0.05 were considered significant.

A total of 24 upregulated genes were identified in LSGs (table 1). These included immunoglobulins, HLAs, complements, TCRs, IFN-inducible proteins, thymosin β and transcriptional factors. We also identified one single downregulated gene, LIM protein. Among the abnormally expressed genes in SS LSG, expression level 19 was significantly higher than in the controls. These included thymosin β4 and thymosin β10, the regulators of apoptosis activity and inflammation-related genes such as HLA-DR and TCRβ. Upregulation of HLA, complements, TCRs and immunoglobulins should be due to the infiltration of T cells and B cells in LSGs from patients with SS. Interestingly, many IFNγ-inducible genes, such as IP10, STAT1α and STAT1β, were highly expressed in SS, and our previous study reported that STAT1 could function as a key molecule in the pathogenesis of SS.[6] These findings suggest that Th1 cells and Th1 type cytokines function as destructive factors in the generation of sialoadenitis in LSGs of patients with SS. Thymosin β has anti-apoptotic activity,[7] suggesting that it may function as a protective factor against salivary gland destruction in patients with SS.

Recent studies reported the presence of germinal centre-like structures in the salivary glands of patients with SS, and that the germinal centre formed by infiltrating mononuclear cells (B cells, T cells and others) produces autoantibodies and exhibits apoptosis.[8 9] In this study, the significant upregulation of 10 genes—for example, IgHCγ, HLA class I, HLA class II, C3 and TCRβ—might be due to mononuclear infiltrates and might be responsible for the formation of a germinal centre, in LSGs of patients with SS.

In conclusion, cDNA microarray analysis demonstrated upregulation of IFNγ-related genes in LSGs of patients with SS, indicating that Th1 cells might play a crucial role in the generation of sialoadenitis in those patients.

Authors' affiliations
Ei Wakamatsu, Yumi Nakamura, Isao Matsumoto, Daisuke Goto, Satoshi Ito, Akito Tsutsumi, Takayuki Sumida, Division of Clinical Immunology, Major of Advanced Biochemical Applications, Graduate School Comprehensive Human Science, University of Tsukuba, Ibaraki, Japan

Competing interests: None declared.

Correspondence to: Professor T Sumida, Division of Clinical Immunology, Major of Advanced Biochemical Applications, Graduate School Comprehensive Human Science, University of Tsukuba, 1-1-1 Tennodai, Tsukuba City, Ibaraki 305-8575, Japan; tsumida@md.tsukuba.ac.jp

Accepted 21 December 2006

REFERENCES

1 **Sumida T,** Matsumoto I, Maeda T, Nishioka K. T-cell receptor in Sjögren's syndrome. *Br J Rheumatol* 1997;36:622–9.
2 **Fox IR,** Kang IH, Ando D, Abrams J, Pisa E. Cytokine mRNA expression in salivary gland biopsies of Sjögren's syndrome. *J Immunol* 1994;152:5532–9.
3 **Ohyama Y,** Nakamura S, Matsuzaki G, Shinohara M, Hiroki A, Fujimura T, *et al.* Cytokine messenger RNA expression in the labial salivary glands of patients with Sjogren's syndrome. *Arthritis Rheum* 1996;39:13769–84.
4 **Hjelmervik TO,** Petersen K, Jonassen I, Jonsson R, Bolstad AI. Gene expression profiling of minor salivary glands clearly distinguishes primary Sjogren's syndrome patients from healthy control subjects. *Arthritis Rheum* 2005;52:1534–44.
5 **Gottenberg JE,** Cagnard N, Lucchesi C, Letourneur F, Mistou S, Lazure T, *et al.* Activation of IFN pathways and plasmacytoid dendritic cell recruitment in target organs of primary Sjogren's syndrome. *Proc Natl Acad Sci USA* 2006;103:2770–5.
6 **Wakamatsu E,** Matsumoto I, Yasukochi T, Naito Y, Goto D, Mamura M, *et al.* Overexpression of phosphorylated STAT1-α in labial salivary glands of patients with Sjogren's syndrome. *Arthritis Rheum* 2006;54:3476–84.
7 **Choi SY,** Kim DK, Eun B, Kim K, Sun W, Kim H. Anti-apoptotic function of thymosin-beta in developing chick spinal motoneurons. *Biochem Biophys Res Commun* 2006;346:872–8.
8 **Amft N,** Curnow SJ, Scheel-Toellner D, Devadas A, Oates J, Crocker J, *et al.* Ectopic expression of the B cell-attracting chemokine BCA-1 (CXCL13) on endothelial cells and within lymphoid follicles contributes to the establishment of germinal center-like structures in Sjogren's syndrome. *Arthritis Rheum* 2001;44:2633–41.
9 **Salomonsson S,** Jonsson MV, Skarstein K, Brokstad KA, Hjelmstrom P, Wahren-Herlenius M, *et al.* Cellular basis of ectopic germinal center formation and autoantibody production in the target organ of patients with Sjogren's syndrome. *Arthritis Rheum* 2003;48:3187–201.

Regression of intestinal adenomas by vaccination with heat shock protein 105-pulsed bone marrow-derived dendritic cells in $Apc^{Min/+}$ mice

Kazunori Yokomine,[1,2] Tetsuya Nakatsura,[1,3] Satoru Senju,[1] Naomi Nakagata,[4] Motozumi Minohara,[5] Jun-ichi Kira,[5] Yutaka Motomura,[1,3] Tatsuko Kubo,[6] Yutaka Sasaki[2] and Yasuharu Nishimura[1,7]

Departments of [1]Immunogenetics and [2]Gastroenterology and Hepatology, Graduate School of Medical Sciences, Kumamoto University, 1-1-1 Honjo, Kumamoto 860-8556; [3]Immunotherapy Section, Investigative Treatment Division Research Center for Innovative Oncology, National Cancer Center Hospital East, 6-5-1 Kashiwanoha, Kashiwa 277-8577; [4]Center for Animal Resources and Development, Kumamoto University, 2-2-1 Honjo, Kumamoto 860-0811; [5]Department of Neurology, Neurological Institute, Graduate School of Medical Sciences, Kyushu University, 3-1-1 Maidashi, Higashi-ku, Fukuoka 812-8582; [6]Department of Molecular Pathology, Graduate School of Medical Sciences, Kumamoto University, 1-1-1 Honjo, Kumamoto 860-8556, Japan

(Received May 12, 2007/Revised August 6, 2007/Accepted August 7, 2007/Online publication September 24, 2007)

Heat shock protein (HSP) 105 is overexpressed in various cancers, but is expressed at low levels in many normal tissues, except for the testis. A vaccination with HSP105-pulsed bone marrow-derived dendritic cells (BM-DC) induced antitumor immunity without causing an autoimmune reaction in a mouse model. Because $Apc^{Min/+}$ mice develop multiple adenomas throughout the intestinal tract by 4 months of age, the mice provide a clinically relevant model of human intestinal tumor. In the present study, we investigated the efficacy of the HSP105-pulsed BM-DC vaccine on tumor regression in the $Apc^{Min/+}$ mouse. Western blot and immunohistochemical analyses revealed that the tumors of the $Apc^{Min/+}$ mice endogenously overexpressed HSP105. Immunization of the $Apc^{Min/+}$ mice with a HSP105-pulsed BM-DC vaccine at 6, 8, and 10 weeks of age significantly reduced the number of small-intestinal polyps accompanied by infiltration of both $CD4^+$ and $CD8^+$ T cells in the tumors. Cell depletion experiments proved that both $CD4^+$ and $CD8^+$ T cells play a critical role in the activation of antitumor immunity induced by these vaccinations. These findings indicate that the HSP105-pulsed BM-DC vaccine can provide potent immunotherapy for tumors that appear spontaneously as a result of the inactivation of a tumor suppressor gene, such as in the $Apc^{Min/+}$ mouse model. (*Cancer Sci* 2007; 98: 1930–1935)

Colorectal cancer is the third most common cancer and the fourth most frequent cause of cancer death worldwide. Every year, more than 945 000 people develop colorectal cancer worldwide, and approximately 492 000 patients die.[1] For patients with advanced stages of colorectal cancer, adjuvant systemic chemotherapy is a standard treatment. Major progress has been made by the introduction of regimens containing new cytotoxic drugs such as irinotecan and oxaliplatin; however, the new therapeutic regimens have led to only 8–9 months of progression-free survival.[2] Consequently, the development of new and effective therapeutic approaches, such as immunotherapy, is needed to expand treatment options.

The progression from normal epithelium to colorectal cancer is a multistep process involving the accumulation of multiple genetic alterations.[3] The *APC* gene, a tumor suppressor, is considered to be a gatekeeper in colon tumorigenesis,[4] and one of the earliest molecular events is the loss of function of the *APC* gene product.[5] APC forms a multimeric complex with the axis inhibition protein (AXIN)2 and glycogen synthase kinase 3β, which regulates the nuclear accumulation of β-catenin, a signal transducer of the wnt pathway.[6] When the APC–β-catenin complex is destabilized because of *APC* mutations, β-catenin binds and activates transcription factors that regulate the expression of potent oncogenes such as *c-Myc* and *c-Met*.[7] The importance of the *APC* gene product was confirmed by the demonstration that 80% of all sporadic colorectal cancers are characterized by one or more mutations in the *APC* gene, approximately 60% of which result in the expression of a truncated version of the APC protein.[8]

The $Apc^{Min/+}$ mouse has a nonsense mutation from T to A in the *Apc* gene at codon 850, homologous to the human germline and somatic *APC* mutation.[9] Although homozygous mice die before birth, all heterozygous mice develop multiple adenomas throughout their intestinal tract at an early age.[10] The $Apc^{Min/+}$ mouse model is unique in that tumors appear spontaneously in the intestinal tract, rather than as a result of induction by a carcinogen. This model is particularly advantageous for testing preventive agents targeted against early stage lesions because adenomas grow to a grossly detectable size within a few months on a defined genetic background.[10] Because $Apc^{Min/+}$ mice develop tumors due to the inactivation of the same tumor suppressor gene known to be involved in the pathogenesis of most colon cancers in humans, this model represents a clinically relevant model of human intestinal tumorigenesis.[10] Furthermore, germline mutations in the human *APC* gene cause FAP, whose symptoms resemble those of an $Apc^{Min/+}$ mouse. Therefore, this model provides useful information about not only colon cancer but also FAP.

Heat shock proteins are soluble intracellular proteins that are expressed ubiquitously, and their expression can be induced at much higher levels due to heat shock or other forms of stress. The essential functions of HSP are to bind and protect partially denatured proteins from further denaturation and aggregation.[11] A previous study reported that HSP105 (often called HSP110), identified with serological identification of antigens using the recombinant expression cloning (SEREX) method, is overexpressed in a variety of human cancers, including colorectal, pancreatic, thyroid, esophageal, and breast carcinoma, whereas HSP105 is expressed at lower levels in many normal tissues, except for the testis.[12,13] Immunotherapy targeted at HSP105 in the mouse prophylactic model, such as HSP105-pulsed BM-DC and *HSP105* DNA vaccines, induce antitumor immunity without causing an autoimmune reaction.[14,15] These findings indicate that HSP105 itself could be considered as a valuable tumor-associated antigen for immune-based treatment of various tumors.

[7]To whom correspondence should be addressed.
E-mail: mxnishim@gpo.kumamoto-u.ac.jp

Abbreviations: APC, adenomatous polyposis coli; BM-DC, bone marrow-derived dendritic cell; COX, cydooxygenase; DC, dendritic cell; ELISPOT, enzyme-linked immunospot; FAP, familial adenomatous polyposis; HSP, heat shock protein; mAb, monodonal antibody; MBP, myelin basic protein; MHC, major histocompatibility complex; PBS, phosphate-buffered saline.

doi: 10.1111/j.1349-7006.2007.00612.x

Another study reported that HSP105 is involved in tumorigenesis by protecting cancer cells from apoptosis.[16] The constitutive overexpression of HSP105 protein was found to be essential for various cancer cells to survive and, conversely, the apoptosis-inducing effect of HSP105 small interfering RNA (siRNA) is specific for cancer. In contrast, HSP can also stimulate an adaptive immune response against antigens bound to HSP,[17] provided that the vaccine forms a complex of recombinant HSP110 and target tumor-associated antigen.[18,19]

In the present study, $Apc^{Min/+}$ mice were used as a model of a cancer immunotherapy for human colorectal cancer. Because tumors in $Apc^{Min/+}$ mice strongly express HSP105, the efficacy of immunization with HSP105-pulsed BM-DC for preventing the development of tumors in $Apc^{Min/+}$ mice was investigated.

Materials and Methods

Mice and genotyping. Frozen embryos of $Apc^{Min/+}$ mice obtained from the Jackson Laboratory were transferred to C57BL/6J mice (purchased from Charles River Japan, Yokohama, Japan) at the Center for Animal Resources and Development, Kumamoto University. Mice at 4–5 weeks of age were characterized for the *Apc* genotype by polymerase chain reaction analysis of tail DNA with the use of allele-specific primers.[20] The concentrations of these primers were 1.0 μM (5′-TGAGAAAGACAGAAGTTA-3′), 1.0 μM (5′-TTCCACTTTGGCATAAGGC-3′), and 0.2 μM (5′-GCCATCCCTTCACGTTAG-3′). The amplification conditions were 5 min at 94°C before 35 cycles at 94°C for 1 min, 50°C for 1 min, and 72°C for 1 min, followed by a final extension at 72°C for 5 min. The mice were maintained by breeding male $Apc^{Min/+}$ mice to female C57BL/6J mice. The mice were kept under specific pathogen-free conditions and these experiments were approved by the Animal Research Committee of Kumamoto University.

Production of recombinant proteins. Highly purified recombinant mouse HSP105 was produced from *Escherichia coli* strain BL21 cells transduced with the mouse *HSP105* gene expression vector, as described previously.[14,21] We also produced highly purified recombinant MBP as a negative control, which was prepared from bacterial lysate in the same way as the preparation of recombinant HSP105. Both recombinant HSP105 and MBP were estimated to be almost endotoxin free using a Limulus amebocyte lysate assay kit (BioWhittaker, Walkersville, MD, USA), and the endotoxin contents in the materials were <10 endotoxin U/mg.

Immunizations and scoring of tumors. HSP105-pulsed BM-DC were prepared as described previously.[14,22] The mice were inoculated intraperitoneally with HSP105-pulsed BM-DC (5×10^5) suspended in 200 μL PBS at 6, 8, and 10 weeks of age. The mice were treated with BM-DC alone, MBP-pulsed BM-DC, or PBS as controls. At 12 weeks of age the mice were killed and their small intestines were removed and fixed with formaldehyde. The intestines were then opened and stained with methylene blue and the number of tumors was counted.

Western blot and immunohistochemical analysis. Western blotting and the immunohistochemical detection of HSP105 were carried out as described previously.[12,16] Rabbit polyclonal antihuman HSP105 (Santa Cruz Biotechnology, Santa Cruz, CA, USA) was used as the primary antibody in this study. The immunohistochemical staining of $CD4^+$ and $CD8^+$ T cells was carried out as described previously.[14] mAb specific to CD4 (L3T4; BD PharMingen, San Diego, CA, USA) and CD8 (Ly-2; BD PharMingen) were used for staining.

Depletion of $CD4^+$ or $CD8^+$ T cells in mice. Rat mAb GK1.5 specific to mouse CD4 and 2.43 specific to mouse CD8 were used to deplete $CD4^+$ and $CD8^+$ T cells, respectively, *in vivo*. The 6-week-old $Apc^{Min/+}$ mice were injected with ascites (500 μg/mouse) from hybridoma-bearing nude mice six times intraperitoneally with an interval of 3–4 days between injection. Normal rat IgG (Chemicon, Temecula, CA, USA) was used as a control. The depletion of T cell subsets was monitored by a flow cytometric analysis, which showed a more than 90% specific depletion in the number of splenocytes.

ELISPOT assay. The $Apc^{Min/+}$ mice were immunized with HSP105-pulsed BM-DC or BM-DC alone at 6 and 8 weeks of age. At 10 weeks of age, spleen cells were harvested and depleted of $CD4^+$ or $CD8^+$ T cells using a magnetic cell-sorting system with antimouse CD4 mAb and antimouse CD8a (Mittenyi Biotec GmbH, Bergisch Gladbach, Germany) mAb, respectively. The purity of these T-cell subsets exceeded 95% based on a flow cytometric analysis. $CD4^-$ T cells were used as a source of $CD8^+$ T cells and antigen-presenting cells, and $CD8^-$ T cells were used as a source of $CD4^+$ T cells and antigen-presenting cells. Five hundred thousand $CD4^-$ or $CD8^-$ T cells were added to each well in triplicate cultures of RPMI-1640 medium containing 10% fetal calf serum (FCS) together with 2 μg/mL HSP105, MBP, and one with medium only at 37°C for 24 h. Then ELISPOT assays were carried out as described previously.[12]

Statistical analysis. The statistical significance of differences between the experimental groups was determined using Student's *t*-test. The overall survival rate was calculated using the Kaplan–Meier method, and statistical significance was evaluated using Wilcoxon's test. A value of $P < 0.05$ was considered to be statistically significant.

Results

Overexpression of HSP105 in intestinal adenomas of the $Apc^{Min/+}$ mice. A previous study reported that mouse HSP105 is overexpressed in liver metastasis of a murine colorectal adenocarcinoma cell line (Colon26), and in lung metastasis of a murine melanoma cell line (B16-F10).[15] The expression of HSP105 in tumors of $Apc^{Min/+}$ mice were thereby analyzed. The small intestines of $Apc^{Min/+}$ mice were excised, and the expression level of HSP105 was evaluated by both western blot and immunohistochemical analyses. The $Apc^{Min/+}$ mice developed adenomatous polyps spontaneously, predominantly in and throughout the small intestine at 4 months of age (Fig. 1a). Both western blot and immunohistochemical analyses confirmed the strong expression of HSP105 in the tumors of $Apc^{Min/+}$ mice (Fig. 1b,c). Based on these observations, the $Apc^{Min/+}$ mouse was chosen as a murine model of cancer immunotherapy targeted at HSP105.

Immunization with HSP105-pulsed BM-DC vaccine reduced the number of small intestinal polyps in $Apc^{Min/+}$ mice. The preventive effects of HSP105-pulsed BM-DC vaccination on the development of adenomatous polyps in the $Apc^{Min/+}$ mice were investigated. The mice were divided into four groups consisting of 10 mice each, inoculated intraperitoneally with PBS (group 1), BM-DC (group 2), MBP-pulsed BM-DC (group 3), or HSP105-pulsed BM-DC (group 4) at 6, 8, and 10 weeks of age. Two weeks after the last immunization, the number of tumors in the small intestine was counted.

Tumors had already developed in the small intestine of $Apc^{Min/+}$ mice at the time of the first vaccination (6 weeks of age). Each mouse had a mean of 6.3 ± 3.4 tumors at that time. The mean number of tumors at 12 weeks of age was 20.9 ± 9.6 in group 4, which was significantly less ($P = 0.006$) than the numbers in group 1 (37.8 ± 11.0), group 2 (40.8 ± 11.0), and group 3 (34.8 ± 9.5) (Fig. 2a). It was therefore concluded that the HSP105-pulsed BM-DC vaccine has the potential to prevent the growth of tumors expressing HSP105. The survival time in group 4 (175.3 ± 32.6 days) tended to be longer than that in group 1 (146.7 ± 13.0 days) and in group 2 (152.7 ± 25.5 days); however, the difference between group 4 and group 2 was not statistically significant ($P = 0.081$; Fig. 2b). No apparent abnormalities, such as weight loss, hair abnormality, or paralysis, were observed in

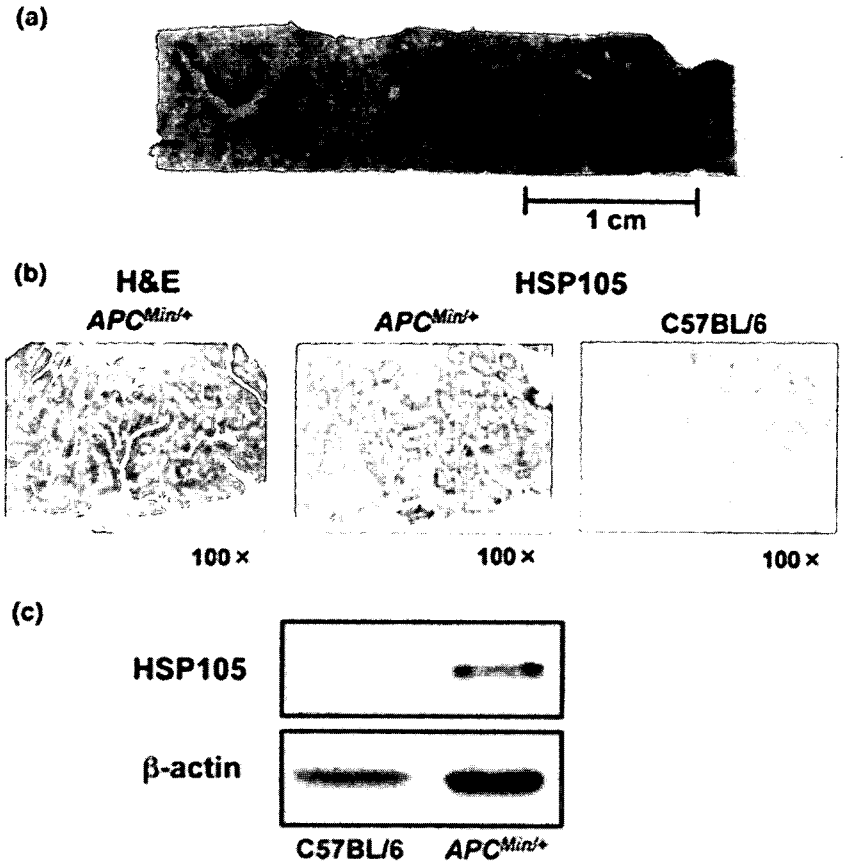

Fig. 1. Overexpression of heat shock protein (HSP) 105 in adenomatous polyps of $Apc^{Min/+}$ mice. (a) Macroscopic polyps in the small intestine of 4-month-old $Apc^{Min/+}$ mice. (b) A microscopic analysis of polyps in the small intestine of 12-week-old $Apc^{Min/+}$ mice stained with hematoxylin-eosin (left) and anti-HSP105 monoclonal antibody (middle). A normal small intestine was stained with anti-HSP105 monoclonal antibody as a negative control (right). Objective magnification was ×100. (c) Western blot analysis of HSP105 in the small intestine of 4-month-old $Apc^{Min/+}$ mice. The samples were small intestines of $Apc^{Min/+}$ and C57BL/6J mice homogenized in lysis buffer. The small intestines of three mice per group were pooled.

the mice immunized with HSP105-pulsed BM-DC, suggesting that serious autoimmunity was not observed in the mice. A histological analysis of the major organs (brain, lung, heart, liver, small intestine, kidney, and testis) of the immunized mice revealed no pathological inflammation (data not shown).

Both CD4⁺ and CD8⁺ T cells are required for antitumor immunity. To determine the role of $CD4^+$ and $CD8^+$ T cells in the reduction of tumor development in $Apc^{Min/+}$ mice immunized with HSP105-pulsed BM-DC, mice were depleted of $CD4^+$ or $CD8^+$ T cells by treatment with anti-CD4 or anti-CD8 mAb, respectively, *in vivo*. During the depletion procedure, the mice were immunized with PBS or HSP105-pulsed BM-DC vaccine (Fig. 3a). In the group of mice immunized with HSP105-pulsed BM-DC, together with inoculation of anti-CD4 mAb (35.5 ± 10.8) or anti-CD8 mAb (30.2 ± 9.6), the tumor numbers were significantly larger than those in the mice given rat IgG (18.8 ± 5.9) or left untreated (19.9 ± 7.7). The differences in the tumor numbers between the anti-CD4 mAb-treated group and the rat IgG-treated group ($P = 0.002$), and between the anti-CD8 mAb-treated group and the rat IgG-treated group ($P = 0.013$) were statistically significant. In the group of mice inoculated with PBS, the numbers of tumors in the mice given either anti-CD4 mAb (38.1 ± 5.7) or anti-CD8 mAb (38.1 ± 5.6) did not differ significantly from those in the mice given rat IgG (37.8 ± 4.8) or in the untreated mice (40.8 ± 6.1) (Fig. 3b). These results suggest that both $CD4^+$ and $CD8^+$ T cells play a crucial role in the protective antitumor immunity induced by the HSP105-pulsed BM-DC vaccine, because the HSP105-pulsed BM-DC vaccine was not effective in the mice showing a depletion of either $CD4^+$ or $CD8^+$ T cells.

Detection of HSP105-specific T cells in mice immunized with the HSP105-pulsed BM-DC vaccine. The $Apc^{Min/+}$ mice were immunized with HSP105-pulsed BM-DC or BM-DC at 6 and 8 weeks of age. At 10 weeks of age, spleen cells were harvested and depleted of $CD4^+$ or $CD8^+$ T cells using magnetic cell-sorting system, and the ELISPOT assay was carried out. The ELISPOT assay showed that the $CD8^-$ cells ($CD4^+$ T cells and antigen-presenting cells) derived from the mice immunized with HSP105-pulsed BM-DC produced a significantly larger amount of interferon-γ in response to HSP105 than did $CD8^-$ cells derived from mice immunized with BM-DC. Similar results were observed for the $CD4^-$ cells ($CD8^+$ T cells and antigen-presenting cells) (Fig. 4a). These observations clearly indicate that both HSP105-specific $CD4^+$ and $CD8^+$ T cells were induced in the mice immunized with HSP105-pulsed BM-DC vaccine.

To investigate the antitumor effect of the HSP105-pulsed BM-DC vaccination, the tumor was evaluated histopathologically. The small intestines derived from the mice used for the ELISPOT assay were stained with anti-CD4 or anti-CD8 mAb. Both $CD4^+$ and $CD8^+$ T cells infiltrated into the tumors of mice immunized with HSP105-pulsed BM-DC; however, this was not the case in tumors derived from the mice immunized with BM-DC (Fig. 4b). These results suggest that HSP105-pulsed BM-DC have the potential to sensitize many HSP105-specific $CD4^+$ and $CD8^+$ T cells to kill tumor cells.

Discussion

In the present study, the HSP105-pulsed BM-DC vaccine could sensitize HSP105-specific T cells *in vivo* and inhibited the spontaneous development of intestinal tumors overexpressing HSP105 in $Apc^{Min/+}$ mice. For diseases of germline mutations that cause malignancy throughout the body, such as FAP, novel strategies for the prevention of cancer are needed urgently because there is no satisfactory treatment for FAP. Therefore,

doi: 10.1111/j.1349-7006.2007.00612.x

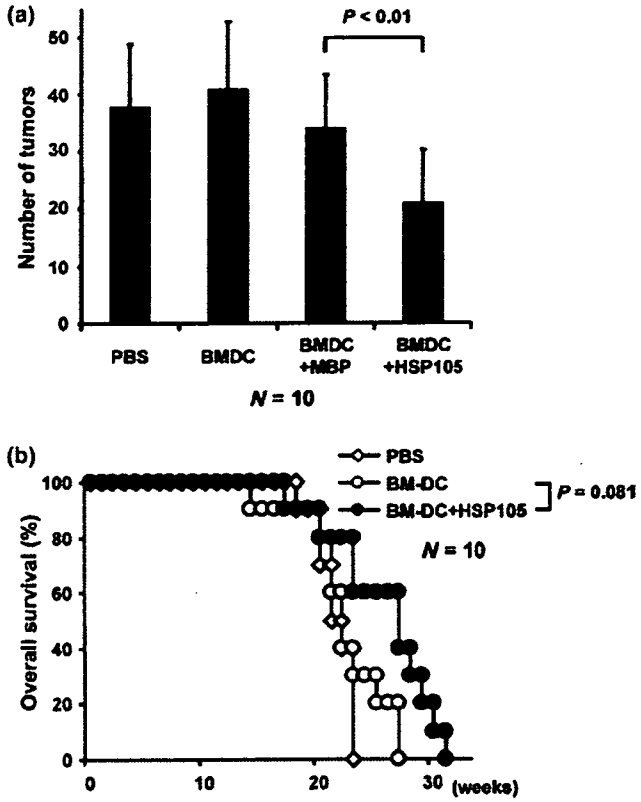

Fig. 2. Vaccination with heat shock protein (HSP) 105-pulsed bone marrow-derived dendritic cells (BM-DC) decreased the number of polyps in the small intestine of the $Apc^{Min/+}$ mice. (a) The $Apc^{Min/+}$ mice were inoculated intraperitoneally with HSP105-pulsed BM-DC (5×10^5), BM-DC alone, or myelin basic protein-pulsed BM-DC or phosphate-buffered saline (PBS) at 6, 8, and 10 weeks of age. At 12 weeks of age, the small intestines of the $Apc^{Min/+}$ mice were excised, stained with methylene blue, and the number of tumors was counted by the naked eye. Each group consisted of 10 $Apc^{Min/+}$ mice. The statistical significance of the differences in results was determined using an unpaired *t*-test. (b) The survival rate of $Apc^{Min/+}$ mice immunized with HSP105-pulsed BM-DC, BM-DC alone, or PBS as a control. The immunization protocol was the same as that of (a). The overall survival rate was calculated using the Kaplan–Meier method, and statistical significance was evaluated using Wilcoxon's test.

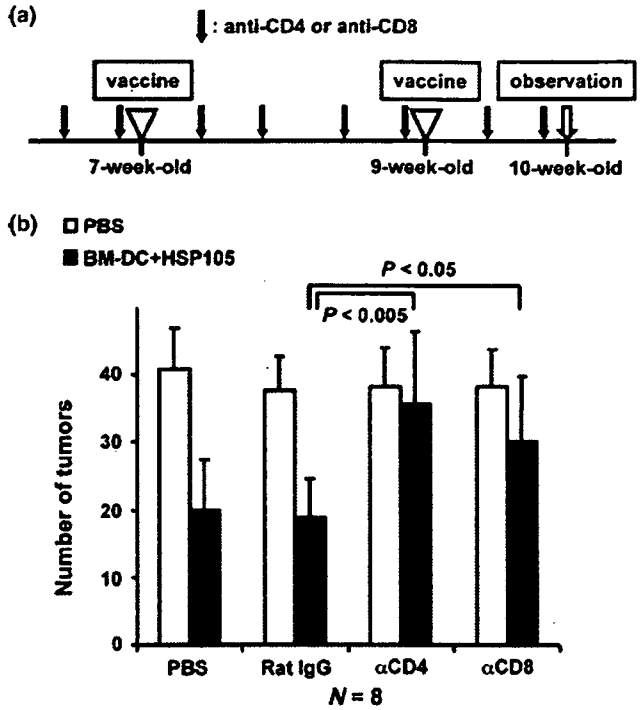

Fig. 3. Both $CD4^+$ and $CD8^+$ T cells are involved in the antitumor immunity elicited by the heat shock protein (HSP) 105-pulsed dendritic cell vaccine. (a) The protocol for the vaccination and the depletion of T cell subsets. (b) The number of polyps in the small intestine of $Apc^{Min/+}$ mice with various treatments. The number of tumors was counted as described in the legend for Fig. 2. Each group consisted of eight $Apc^{Min/+}$ mice. The statistical significance of the difference between the results was determined using the unpaired *t*-test.

the specific objective of the present study was to find out whether HSP105-pulsed DC-based immunotherapy can be used as a potent new strategy for the prevention of spontaneously arising tumors in FAP patients.

The ELISPOT assay shown in Figure 4a shows that both $CD4^+$ and $CD8^+$ HSP105-reactive T cells were primed in the mice immunized with HSP105-pulsed BM-DC. In this assay, we cannot completely rule out the possibility that responses were directed against contaminated bacteria-derived molecules in the HSP105 recombinant protein preparation. However, we consider this unlikely because practically no response was observed against BM-DC loaded with recombinant MBP protein, which was prepared from bacterial lysate in the same way as the preparation of recombinant HSP105. These recombinant proteins were purified extensively as described in a previous paper,[14] and contamination of lipopolysaccharide (LPS) or other DC-stimulants was ruled out.

Previous studies have reported that HSP105 is overexpressed specifically in a variety of human cancers and mouse tumor cells.[13,14] The present study demonstrated that HSP105 was also strongly expressed in the adenomatous polyps of $Apc^{Min/+}$ mice. In human tissue, the overexpression of HSP105 is a late event in the adenoma–carcinoma sequence, because immunohistochemical analysis revealed that HSP105 is strongly expressed in adenocarcinoma but not in adenoma.[13] Although the $Apc^{Min/+}$ mouse model has provided useful information about the pathogenesis of colorectal cancer, it is limited because it does not completely mimic the disease in humans. In humans, patients with FAP develop hundreds to thousands of adenomatous polyps, predominantly in the distal colon, and have a high risk of malignancies before the age of 40 years.[23] In contrast, $Apc^{Min/+}$ mice develop dozens to hundreds of adenomas and have a shortened life span. However, these adenomas are located mainly in the small intestine and they generally do not become malignant.[10] Furthermore, mice carrying different *Apc* mutations have been established. Tumors arising in these mice are histologically similar, but vary with respect to age of onset, number of tumors, and location.[24] Given this variation, the pattern of HSP105 expression in intestinal tumors may be different between human and $Apc^{Min/+}$ mice. Regardless of these differences, the $Apc^{Min/+}$ mice provide an appropriate model for analysis of the efficacy of the HSP105-pulsed BM-DC vaccine for inhibition of the development of human colorectal cancer, because the loss of *APC* function is the initiating event in not only FAP but also in the vast majority of sporadic colon cancers.

Recent findings regarding the cellular and molecular pathogenesis of colorectal cancer have led to the development of new targeted therapeutic options. Overexpression of COX-2 is one of the most significant observations in this respect.[25] The use of COX-2 inhibitor suppresses the development of colon cancer in

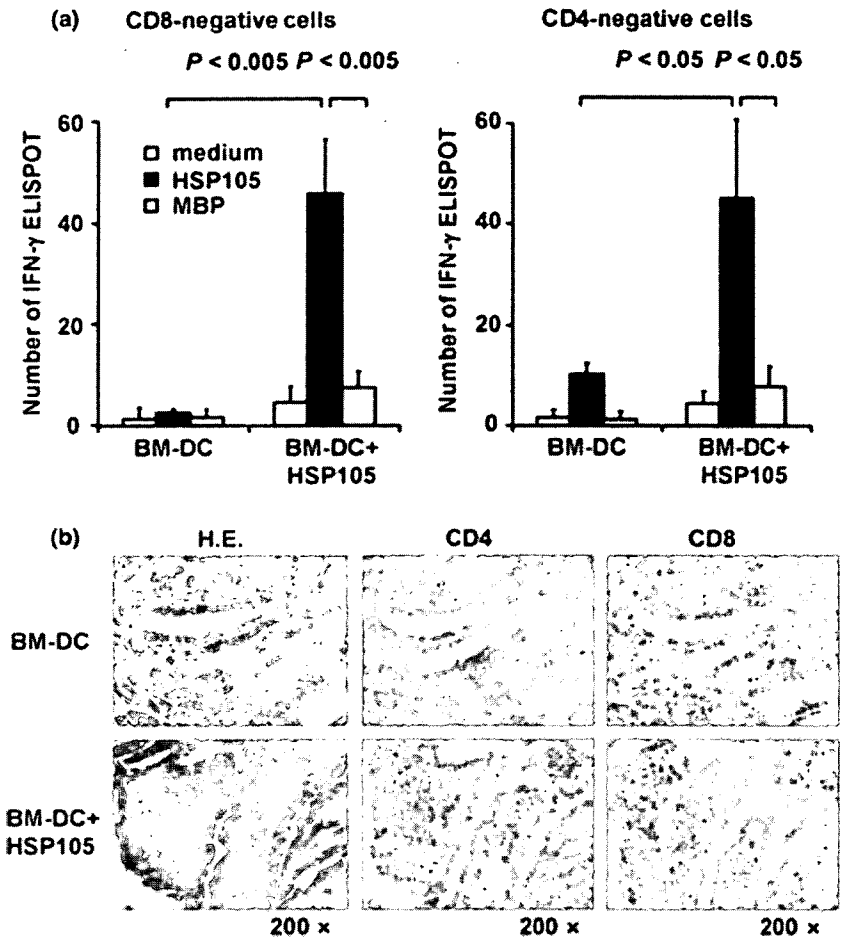

Fig. 4. Induction of heat shock protein (HSP) 105-specific T cells via immunization with HSP105-pulsed bone marrow-derived dendritic cells (BM-DC). (a) The $Apc^{Min/+}$ mice were inoculated with HSP105-pulsed BM-DC or BM-DC at 6 and 8 weeks of age. The spleen cells were harvested from 10-week-old $Apc^{Min/+}$ mice and depleted with either $CD4^+$ or $CD8^+$ cells using magnetic cell-sorting system. $CD4^-$ cells were used as a source of $CD8^+$ T cells and antigen-presenting cells, and $CD8^-$ cells were used as a source of $CD4^+$ T cells and antigen-presenting cells. Thereafter interferon-γ enzyme-linked immunospot (ELISPOT) assays were carried out. Briefly, $CD4^-$ or $CD8^-$ T cells (5×10^5) in each well were cultured together with 2 μg/mL HSP105, myelin basic protein, or medium alone for 24 h. The statistical significance of the difference in results was determined using the unpaired *t*-test. The spleens of three mice from each group were pooled. This experiment was carried out three times, with similar results. (b) The $Apc^{Min/+}$ mice were inoculated with HSP105-pulsed BM-DC or BM-DC at 6 and 8 weeks of age. The small intestines were excised from 10-week-old $Apc^{Min/+}$ mice and then were analyzed after immunohistochemical staining with anti-CD4 monoclonal antibody or anti-CD8 monoclonal antibody (magnification ×200).

sporadic cases[26] and FAP;[27] however, recent clinical trials suggest that the use of high doses of COX-2 inhibitor may have dangerous side-effects, such as increased risk of cardiovascular disease.[28] In the present study, no apparent autoimmunity was observed in the $Apc^{Min/+}$ mice immunized with HSP105-pulsed BM-DC, an observation similar to our previous findings.[14,22] In some human clinical trials of DC-based cancer immunotherapy, even in patients with advanced stages of cancer, no major toxicity nor severe side-effects were observed.[29–31] These results strongly suggest that DC-based immunotherapy is safe and feasible.

DC vaccination is now considered to be one of the most promising strategies for cancer immunotherapy.[32,33] DC are the most potent antigen-presenting cells and can present tumor antigens to stimulate a tumor-specific T-cell response. However, this does not occur in most types of cancer and in animal models of spontaneously arising tumors.[34] In the present study, immunization with HSP105-pulsed BM-DC vaccine significantly reduced the number of small-intestinal polyps in the $Apc^{Min/+}$ mice; however, the duration of survival was not prolonged as had been expected because the adenomas in $Apc^{Min/+}$ mice generally did not become malignant. Thereby, the protocol of DC-based vaccination used in the present study was not sufficient to completely prevent the occurrence of the tumors *in vivo*, and we are trying to establish a more effective immunization protocol. New strategies are now being developed to improve the clinical efficacy of DC-based vaccines, for example, the use of overexpression of Akt1 in BM-DC, suppressor of cytokine signaling 1-silenced BM-DC, and CD40-inducible DC.[35–37] The use of transfected DC in a protocol such as that used in the present study has the potential to induce a more effective antitumor response. Furthermore, it is necessary to investigate whether combinations of immunotherapy and other therapies, such as combinations of DC vaccines and chemotherapy or low-dose COX-2 inhibitors, induce a more effective antitumor response in comparison to individual therapy alone, thereby developing more effective strategies for treating colorectal cancer. Recent findings have shown the curative potential of combinations of irradiation,[38] chemotherapy,[39] and subsequent adoptive T-cell immunotherapy against established solid tumors.[40]

The abrogation of the antitumor effect of the HSP105-pulsed BM-DC vaccine, after the depletion of $CD4^+$ cells or $CD8^+$ cells via the administration of mAb, indicates that both $CD4^+$ and $CD8^+$ T cells play a critical role in the antitumor effect of HSP105-pulsed BM-DC. The report that antigen-specific $CD4^+$ T helper cells are required for the activation of $CD8^+$ effector T cells, their secondary expansion, and memory induction,[41] is consistent with the findings that $CD4^+$ T cells played an important role in tumor rejection in the present study. Peptides derived from HSP105 incorporated into BM-DC might be presented in the context of MHC class II on the surface of BM-DC to activate $CD4^+$ T cells. Subsequently, $CD4^+$ T cells produce interferon-γ and interleukin-2 to activate HSP105-specific $CD8^+$ effector T cells and facilitate the development of HSP105-specific $CD8^+$ memory T cells. Furthermore, the ELISPOT assay showed that HSP105-specific $CD8^+$ T cells were also activated by HSP105-pulsed antigen-presenting cells. These results indicate

doi: 10.1111/j.1349-7006.2007.00612.x

that HSP105-pulsed BM-DC can demonstrate peptides derived from exogenously added HSP105 not only in the context of MHC class II molecules to activate $CD4^+$ T cells but also in the context of MHC class I molecules via the mechanism of cross-presentation to activate $CD8^+$ T cells. Whole-protein-pulsed DC vaccines seem to be superior to peptide-pulsed DC because they can activate both $CD4^+$ and $CD8^+$ T cells, and it does not require a knowledge of the human leukocyte antigen (HLA) type of the cancer patients.

In conclusion, the results of the present study indicate that HSP105-pulsed BM-DC may provide a potential vaccine to combat human colorectal cancer. It is possible that immunization with HSP105-pulsed BM-DC vaccines could be useful in patients with colorectal cancer to prevent tumor recurrence after surgical resection. Although there was a noteworthy effect of this type of vaccine on the host immune response to tumors expressing HSP105, further investigation to improve the clinical efficacy of HSP105-pulsed BM-DC vaccines is called for.

Acknowledgments

This work was supported in part by Grants-in-Aid (no. 12213111 for Y. Nishimura, no. 14770142 for T. Nakatsura, and no. 14770142 for S. Senju) from the Ministry of Education, Science, Technology, Sports, and Culture, Japan, and The Sagawa Foundation for Promotion of Cancer Research and Meiji Institute of Health Science.

References

1 Weitz J, Koch M, Debus J, Hohler T, Galle PR, Büchler MW. Colorectal cancer. *Lancet* 2005; 365: 153–65.
2 Tournigand C, André T, Achille E *et al.* FOLFIRI followed by FOLFOX6 or the reverse sequence in advanced colorectal cancer: a randomized GERCOR study. *J Clin Oncol* 2004; 22: 229–37.
3 Rao CV, Cooma I, Rosa Rodriguez JG, Simi B, El-Bayoumy K, Reddy BS. Chemoprevention of familial adenomatous polyposis development in the *Apc*^{min} mouse model by 1,4-phenylene *bis*(methylene)selenocyanate. *Carcinogenesis* 2000; 21: 617–21.
4 Kinzler KW, Vogelstein B. Cancer-susceptibility genes: gatekeepers and caretakers. *Nature* 1997; 386: 761–3.
5 Fearon ER, Vogelstein B. A genetic model for colorectal tumorigenesis. *Cell* 1990; 61: 759–67.
6 Kikuchi A. Modulation of Wnt signaling by Axin and Axil. *Cytokine Growth Factor Rev* 1999; 10: 255–65.
7 Sancho E, Batlle E, Clevers H. Signaling pathways in intestinal development and cancer. *Annu Rev Cell Dev Biol* 2004; 20: 695–723.
8 Miyoshi Y, Ando H, Nagase H *et al.* Germ-line mutations of the *APC* gene in 53 familial adenomatous polyposis patients. *Proc Natl Acad Sci USA* 1992; 89: 4452–6.
9 Su LK, Kinzler KW, Vogelstein B *et al.* Multiple intestinal neoplasia caused by a mutation in the murine homolog of the *APC* gene. *Science* 1992; 256: 668–70.
10 Moser AR, Pitot HC, Dove WF. A dominant mutation that predisposes to multiple intestinal neoplasia in the mouse. *Science* 1990; 247: 322–4.
11 Feder ME, Hofmann GE. Heat-shock proteins, molecular chaperones, and the stress response: evolutionary and ecological physiology. *Annu Rev Physiol* 1999; 61: 243–82.
12 Nakatsura T, Senju S, Yamada K, Jotsuka T, Ogawa M, Nishimura Y. Gene cloning of immunogenic antigens overexpressed in pancreatic cancer. *Biochem Biophys Res Commun* 2001; 281: 936–44.
13 Kai M, Nakatsura T, Egami H, Senju S, Nishimura Y, Ogawa M. Heat shock protein 105 is overexpressed in a variety of human tumors. *Oncol Rep* 2003; 10: 1777–82.
14 Yokomine K, Nakatsura T, Minohara M *et al.* Immunization with heat shock protein 105-pulsed dendritic cells leads to tumor rejection in mice. *Biochem Biophys Res Commun* 2006; 343: 269–78.
15 Miyazaki M, Nakatsura T, Yokomine K *et al.* DNA vaccination of HSP105 leads to tumor rejection of colorectal cancer and melanoma in mice through activation of both $CD4^+$ T cells and $CD8^+$ T cells. *Cancer Sci* 2005; 96: 695–705.
16 Hosaka S, Nakatsura T, Tsukamoto H, Hatayama T, Baba H, Nishimura Y. Synthetic small interfering RNA targeting heat shock protein 105 induces apoptosis of various cancer cells both *in vitro* and *in vivo*. *Cancer Sci* 2006; 97: 623–32.
17 Srivastava P. Interaction of heat shock proteins with peptides and antigen presenting cells: chaperoning of the innate and adaptive immune responses. *Annu Rev Immunol* 2002; 20: 395–425.
18 Manjili MH, Wang XY, Chen X *et al.* HSP110–HER2/neu chaperone complex vaccine induces protective immunity against spontaneous mammary tumors in HER-2/neu transgenic mice. *J Immunol* 2003; 171: 4054–61.
19 Wang XY, Chen X, Manjili MH, Repasky E, Henderson R, Subjeck JR. Targeted immunotherapy using reconstituted chaperone complexes of heat shock protein 110 and melanoma-associated antigen gp100. *Cancer Res* 2003; 63: 2553–60.
20 Dietrich WF, Lander ES, Smith JS *et al.* Genetic identification of *Mom*-1, a major modifier locus affecting *Min*-induced intestinal neoplasia in the mouse. *Cell* 1993; 75: 631–9.
21 Yamagishi N, Nishihori H, Ishihara K, Ohtsuka K, Hatayama T. Modulation of the chaperone activities of Hsc70/Hsp40 by Hsp105α and Hsp105β. *Biochem Biophys Res Commun* 2000; 272: 850–5.
22 Nakatsura T, Komori H, Kubo T *et al.* Mouse homologue of a novel human oncofetal antigen, glypican-3, evokes T-cell-mediated tumor rejection without autoimmune reaction in mice. *Clin Cancer Res* 2004; 10: 8630–40.
23 Fearnhead NS, Wilding JL, Bodmer WF. Genetics of colorectal cancer: hereditary aspects and overview of colorectal tumorigenesis. *Br Med Bull* 2002; 64: 27–43.
24 Boivin GP, Washington K, Yang K *et al.* Pathology of mouse models of intestinal cancer: consensus report and recommendations. *Gastroenterology* 2003; 124: 762–77.
25 Oshima M, Dinchuk JE, Kargman SL *et al.* Suppression of intestinal polyposis in *Apc* Δ716 knockout mice by inhibition of cyclooxygenase 2 (COX-2). *Cell* 1996; 87: 803–9.
26 Reddy BS, Hirose Y, Lubet R *et al.* Chemoprevention of colon cancer by specific cyclooxygenase-2 inhibitor, celecoxib, administered during different stages of carcinogenesis. *Cancer Res* 2000; 60: 293–7.
27 Steinbach G, Lynch PM, Philips RKS *et al.* The effect of celecoxib, a cyclooxygenase-2 inhibitor, in familial adenomatous polyposis. *N Engl J Med* 2000; 342: 1946–52.
28 Solomon SD, McMurray JJV, Pfeffer MA *et al.* Cardiovascular risk associated with celecoxib in a clinical trial for colorectal adenoma prevention. *N Engl J Med* 2005; 352: 1071–80.
29 Nestle FO, Alijagic S, Gilliet M *et al.* Vaccination of melanoma patients with peptide- or tumor lysate-pulsed dendritic cells. *Nat Med* 1998; 4: 328–32.
30 Stift A, Friedl J, Dubsky P *et al.* Dendritic cell-based vaccination in solid cancer. *J Clin Oncol* 2003; 21: 135–42.
31 Yu JS, Liu G, Ying H, Yong WH, Black KL, Wheeler CJ. Vaccination with tumor lysate-pulsed dendritic cells elicits antigen-specific, cytotoxic T-cells in patients with malignant glioma. *Cancer Res* 2004; 64: 4973–9.
32 Timmerman JM, Levy R. Dendritic cell vaccines for cancer immunotherapy. *Annu Rev Med* 1999; 50: 507–29.
33 Fong L, Engleman EG. Dendritic cells in cancer immunotherapy. *Annu Rev Immunol* 2000; 18: 245–73.
34 Gabrilovich D. Mechanisms and functional significance of tumour-induced dendritic-cell defects. *Nature Rev Immunol* 2004; 4: 941–52.
35 Park D, Lapteva N, Seethammagari M, Slawin KM, Spencer D. An essential role for Akt1 in dendritic cell function and tumor immunotherapy. *Nat Biotechnol* 2006; 24: 1581–90.
36 Evel-Kabler K, Song XT, Aldrich M, Huang XF, Chen SY. SOCS1 restricts dendritic cells' ability to break self tolerance and induce antitumor immunity by regulating IL-12 production and signaling. *J Clin Invest* 2006; 116: 90–100.
37 Hanks BA, Jiang J, Singh RAK *et al.* Re-engineered CD40 receptor enables potent pharmacological activation of dendritic-cell cancer vaccines *in vivo*. *Nat Med* 2005; 11: 130–7.
38 Reits EA, Hodge JW, Herberts CA *et al.* Radiation modulates the peptide repertoire, enhances MHC class I expression, and induces successful antitumor immunotherapy. *J Exp Med* 2006; 203: 1259–71.
39 Casares N, Pequignot MO, Tesniere A *et al.* Caspase-dependent immnogenicity of doxorubicin-induced tumor cell death. *J Exp Med* 2005; 202: 1691–701.
40 Zhang B, Bowerman NA, Salama JK *et al.* Induced sensitization of tumor stroma leads to eradication of established cancer by T cells. *J Exp Med* 2007; 204: 49–55.
41 Janssen EE, Lemmens EE, Wolfe T, Christen U, von Herrath MG, Schoenberger SP. $CD4^+$ T cells are required for secondary expansion and memory in $CD8^+$ T lymphocytes. *Nature* 2003; 421: 852–6.

STEM CELLS

EMBRYONIC STEM CELLS

Genetically Manipulated Human Embryonic Stem Cell-Derived Dendritic Cells with Immune Regulatory Function

SATORU SENJU,[a] HIROFUMI SUEMORI,[b] HITOSHI ZEMBUTSU,[c] YASUSHI UEMURA,[a] SHINYA HIRATA,[a] DAIKI FUKUMA,[a] HIDETAKE MATSUYOSHI,[a] MANAMI SHIMOMURA,[a] MIWA HARUTA,[a] SATOSHI FUKUSHIMA,[a] YUSUKE MATSUNAGA,[a] TOYOMASA KATAGIRI,[c] YUSUKE NAKAMURA,[c] MASATAKA FURUYA,[b] NORIO NAKATSUJI,[d] YASUHARU NISHIMURA[a]

[a]Department of Immunogenetics, Graduate School of Medical and Pharmaceutical Sciences, Kumamoto University, Kumamoto, Japan; [b]Laboratory of Embryonic Stem Cell Research, Stem Cell Research Center, Institute for Frontier Medical Sciences, Kyoto University, Kyoto, Japan; [c]Laboratory of Molecular Medicine, Human Genome Center, Institute of Medical Science, University of Tokyo, Tokyo, Japan; [d]Department of Development and Differentiation, Institute for Frontier Medical Sciences, Kyoto University, Kyoto, Japan

Key Words. Dendritic cells • Embryonic stem cells • Cell differentiation • Cell therapy

ABSTRACT

Genetically manipulated dendritic cells (DC) are considered to be a promising means for antigen-specific immune therapy. This study reports the generation, characterization, and genetic modification of DC derived from human embryonic stem (ES) cells. The human ES cell-derived DC (ES-DC) expressed surface molecules typically expressed by DC and had the capacities to stimulate allogeneic T lymphocytes and to process and present protein antigen in the context of histocompatibility leukocyte antigen (HLA) class II molecule. Genetic modification of human ES-DC can be accomplished without the use of viral vectors, by the introduction of expression vector plasmids into undifferentiated ES cells by electroporation and subsequent induction of differentiation of the transfectant ES cell clones to ES-DC. ES-DC introduced with invariant chain-based antigen-presenting vectors by this procedure stimulated HLA-DR-restricted antigen-specific T cells in the absence of exogenous antigen. Forced expression of programmed death-1-ligand-1 in ES-DC resulted in the reduction of the proliferative response of allogeneic T cells cocultured with the ES-DC. Generation and genetic modification of ES-DC from nonhuman primate (cynomolgus monkey) ES cells was also achieved by the currently established method. ES-DC technology is therefore considered to be a novel means for immune therapy. STEM CELLS *2007;25:2720–2729*

Disclosure of potential conflicts of interest is found at the end of this article.

INTRODUCTION

Embryonic stem (ES) cells are characterized by pluripotency and infinite propagation capacity, and the methods for genetic modification of ES cells, including targeted gene modification, have been well-established. This laboratory and others have devised methods to generate dendritic cells (DC) in vitro from mouse ES cells [1, 2]. The functions of mouse ES cell-derived DC (ES-DC), including stimulation of allogeneic T cells, processing and presentation of antigenic proteins, and migration upon in vivo transfer, are comparable to those of DC generated in vitro from bone marrow cells [3]. This laboratory has also established a strategy for the genetic modification of mouse ES-DC [1]. Expression vectors were introduced into ES cells by electroporation, and subsequently the transfectant ES cell clones were induced to differentiate to ES-DC. Studies using mice have demonstrated that in vivo transfer of genetically engineered mouse ES-DC is very useful for modulating immune responses both positively and negatively. It is possible to induce anticancer immunity [3–6] and prevent autoimmune disease [7, 8] in mouse models with genetically engineered ES-DC.

In the present study, looking toward future clinical application of ES-DC technology, a method was developed to generate ES-DC from human ES cells. The morphology and the results of functional and flow cytometric analyses indicate that human ES-DC possess the characteristic features of DC. cDNA microarray analysis revealed that the change of gene expression profile during generation and maturation of human ES-DC partially mimics that of monocyte-derived DC (Mo-DC). The currently established method was also applicable to cynomolgus monkey (*Macaca fascicularis*) ES cells.

MATERIALS AND METHODS

Cell Lines, Cytokines, and Reagents

The use of human ES cells was done in accordance with the Guidelines for Derivation and Utilization of Human Embryonic Stem Cells (2001) of the Ministry of Education, Culture, Sports, Science and Technology (MEXT), Japan, after approval by the Institutional Review Board. The human ES cell lines KhES-1 and KhES-3 have recently been established and maintained on mouse

Correspondence: Satoru Senju, M.D., Ph.D., Department of Immunogenetics, Graduate School of Medical and Pharmaceutical Sciences, Kumamoto University, 1-1-1 Honjo, Kumamoto 860-8556, Japan. Telephone: 81-96-373-5313; Fax: 81-96-373-5314; e-mail: senjusat@gpo.kumamoto-u.ac.jp Received April 30, 2007; accepted for publication July 27, 2007; first published online in STEM CELLS *EXPRESS* August 9, 2007. 1066-5099/2007/$30.00/0 doi: 10.1634/stemcells.2007-0321

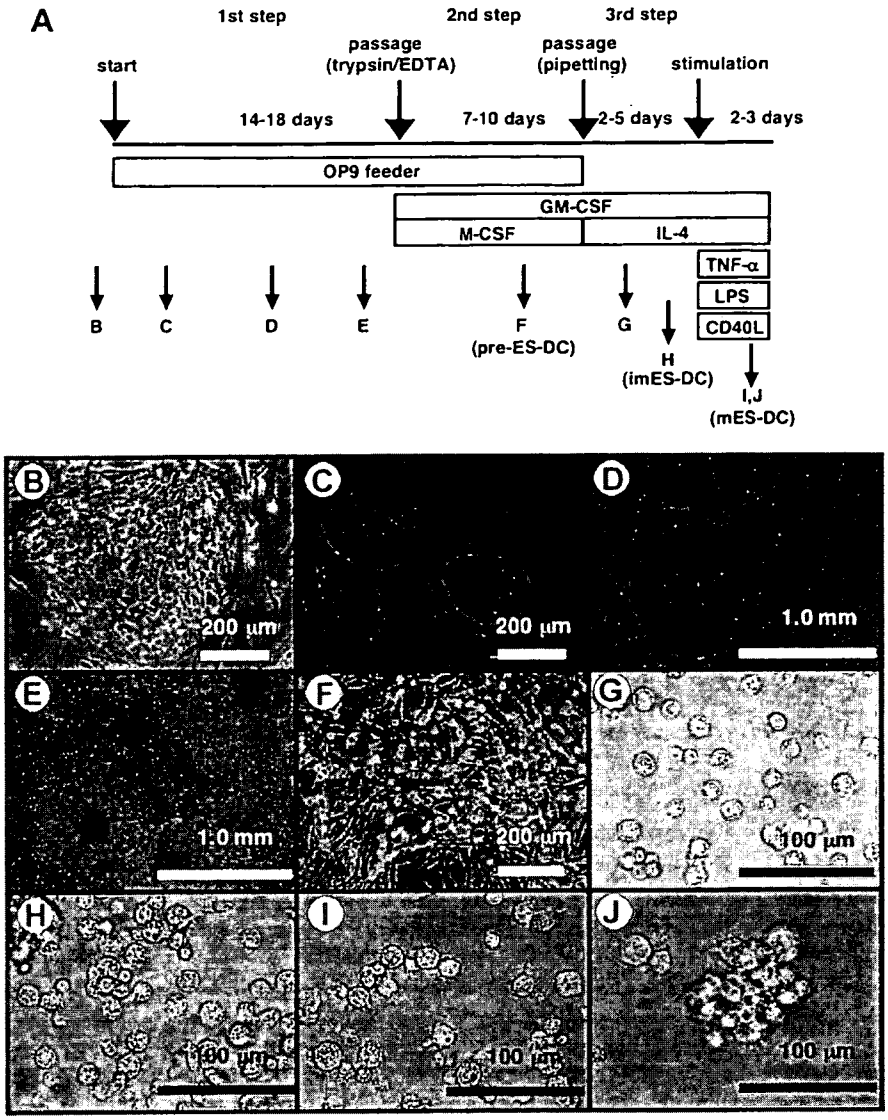

Figure 1. Culture protocol and morphological changes of human embryonic stem (ES) cell-derived cells during differentiation culture. **(A)**: The schedule for the culture to induce differentiation of human ES cells into ES-DC is schematically depicted. **(B)**: Undifferentiated human ES cells on primary embryonic fibroblast feeder layer. **(C–E)**: ES cell-derived cells on day 3 **(C)**, day 11 **(D)**, and day 15 **(E)** in the first step. **(F)**: Cells on day 6 in the second step. **(G–J)**: Cells on day 1 **(G)**, day 3 **(H)**, and day 6 **(I, J)** in the third step. Cells shown in **(I, J)** had been stimulated with TNF-α plus LPS for 2 days. Abbreviations: ES-DC, embryonic stem cell-derived dendritic cells; GM-CSF, granulocyte macrophage colony-stimulating factor; IL, interleukin; imES-DC, immature embryonic stem cell-derived dendritic cells; LPS, lipopolysaccharide; M-CSF, macrophage colony-stimulating factor; mES-DC, mature embryonic stem cell-derived dendritic cells; TNF-α, tumor necrosis factor α.

primary embryonic fibroblast (PEF) feeder layers as previously described [9, 10]. Mouse-derived hematopoietic stromal cell line OP9 was treated with mitomycin C (10 μg/ml) for 1 hour before plating onto gelatin-coated tissue culture dishes to make feeder cell layers. The establishment and maintenance of cynomolgus monkey ES cell line CMK6 was also reported [11, 12]. Recombinant human granulocyte macrophage colony-stimulating factor (GM-CSF), macrophage colony-stimulating factor (M-CSF), interleukin-4 (IL-4), tumor necrosis factor α (TNF-α), and soluble CD40-ligand were purchased from Peprotech (London, http://www.peprotech.com). Lipopolysaccharide (LPS) from *Escherichia coli* and OK-432 were purchased from Sigma-Aldrich (St. Louis, http://www.sigmaaldrich.com) and Chugai Pharmaceutical (Tokyo, http://www.chugai-pharm.co.jp/hc/chugai_top_en.jsp), respectively.

Induction of Differentiation of ES Cells into ES-DC

The procedure for differentiation culture was composed of three steps (Fig. 1A). Step 1 was as follows: undifferentiated ES cells maintained on PEF were rinsed with phosphate-buffered saline (PBS) and treated with dissociation solution containing 1 mg/ml collagenase, 0.25% trypsin, and 20% knockout serum replacement (Invitrogen, Carlsbad, CA, http://www.invitrogen.com) in PBS [10] and cultured on OP9 feeder cell layers in minimum essential medium-α supplemented with 20% fetal calf serum (FCS) and 2-mercaptoethanol (50 μM). Culture of cells was continued for 14–18 days with human ES cells and for 11–13 days with cynomolgus monkey ES cells, and the medium was changed once every 3 days. At the end of this step, the cells were rinsed with PBS, treated with trypsin-EDTA (PBS containing 0.25% trypsin and 1 mM EDTA) for 30–40 minutes, and recovered. After resuspension in culture medium, the cells were plated onto culture dishes and incubated for 2–4 hours. Thereafter, floating or weakly adherent cells were recovered by pipetting, and any firmly adherent cells were discarded. Step 2 was as follows: after being passaged through nylon mesh (Cell Strainer 100 μm; BD Biosciences, Bedford, MA, http://www.bdbiosciences.com), cells recovered from one 90-mm dish were plated in two dishes with freshly prepared OP9 feeder layers. On the following day, the culture medium was exchanged with a medium containing GM-CSF (100 ng/ml) and M-CSF (50 ng/ml). The culture was continued for 7–10 days, depending on the propagation of floating cells on the feeder layers. Step 3 was as follows: ES cell-derived floating cells were recovered by pipetting; resuspended in RPMI 1640 medium containing 10% FCS, GM-CSF (100 ng/ml), and IL-4 (10 ng/ml); and cultured in Petri dishes ($3–5 \times 10^5$ cells per dish) without a feeder layer (Locus, Tokyo). To induce maturation, IL-4 (10 ng/ml), TNF-α (10 ng/ml), LPS (3 μg/ml), and, in some experiments, soluble CD40-ligand (20 ng/ml) or OK-432 (10 μg/ml) were simultaneously added on day 3 or 5 of this step, and the culture was continued for an additional 2–3 days. Differentiating cells were microscopically analyzed on an inverted microscope (IX70; Olympus, Tokyo, http://www.olympus-global.com).

Flow Cytometric Analysis

The following monoclonal antibodies (Ab) conjugated with fluorescein isothiocyanate or phycoerythrin were purchased from BD Pharmingen (San Diego, http://www.bdbiosciences.com/index_us.shtml) or eBioscience Inc. (San Diego, http://www.ebioscience.com): anti-human histocompatibility leukocyte antigen (HLA)-DR (clone L243, mouse IgG2a); anti-HLA-A, B, and C (clone G46-2.6, mouse IgG1); anti-human CD80 (clone L307.4, mouse IgG1); anti-human CD83 (clone HB15e, mouse IgG1); anti-human CD86 (clone FUN-1, mouse IgG1); anti-human CD40 (clone 5C3, mouse IgG1); anti-human B7-H1/programmed death-1-ligand-1 (PD-L1) (clone MIH1, mouse IgG1); and anti-human CD74 (clone M-B741, mouse IgG2a). As isotype-matched controls, mouse IgG2a (clone G155-178) and mouse IgG1 (clone MOPC-21) were used. The cell samples were treated with FcR-blocking reagent (Miltenyi Biotec, Bergisch Gladbach, Germany, http://www.miltenyibiotec.com) for 10 minutes, stained with the fluorochrome-conjugated Ab for 30 minutes, and washed three times with PBS/2% FCS. Intracellular staining with anti-CD74 monoclonal Ab was done by using IntraPrep (Beckman Coulter, Marseille, France, http://www.beckmancoulter.com). Stained cell samples were analyzed on a FACScan flow cytometer, and, in some experiments, the DC fraction was gated by forward and side scatters.

Enzyme-Linked Immunosorbent Assay to Detect Cytokine Production by ES-DC

Cells were cultured in 96-well flat-bottomed culture plates (1.2×10^5 cells in 150 μl of medium per well) in the presence or absence of soluble CD40-ligand, LPS, or OK432. After 60 hours of culture, supernatant was collected, and the concentration of TNF-α and IL-12 p70 was measured by using enzyme-linked immunosorbent assay (ELISA) kits (Pierce, Rockford, IL, http://www.piercenet.com).

Allogeneic T-Cell-Stimulation Assay

Mononuclear cells were isolated from heparinized peripheral blood of a human or a cynomolgus monkey housed in the Chemo-Sero-Therapeutic Research Institute (Kumamoto, Japan), using Ficoll-Paque PLUS (Amersham Biosciences, Uppsala, Sweden, http://www.amersham.com). T cells were purified using the Pan T cell isolation kit for humans or the kit for nonhuman primates (Miltenyi Biotec). The T cells (4×10^4/well) were cocultured with graded numbers of x-ray-irradiated (40 Gy) stimulator cells in RPMI 1640 medium supplemented with 10% human plasma in 96-well round-bottomed culture plates for 5 days. [^{3}H]-Methyl-thymidine (247.9 GBq/mmol) was added to the culture (0.037 MBq/well) for the last 16 hours. At the end this time, the cells were harvested onto glass fiber filters (PerkinElmer Life and Analytical Sciences, Boston, http://www.perkinelmer.com), and the incorporation of [^{3}H]-thymidine was measured by scintillation counting. In the experiment using PD-L1-transfectant ES-DC, anti-PD-L1 blocking Ab (clone MIH1; eBioscience) or control mouse IgG1 Ab (eBioscience) was added to the culture (10 μg/ml).

Recombinant Antigenic Protein

A DNA fragment encoding human glutamic acid decarboxylase (GAD65) p96-174 protein fragment was cloned into the prokaryotic expression vector pGEX-4T-3 (Amersham Biosciences), to generate a vector for glutathione *S*-transferase-fused GAD65 protein fragment (GST-GAD). The induction of the production of recombinant protein in *E. coli* (DH5α) and the extraction of the recombinant protein from bacterial inclusion bodies was done according to Frangioni and Neel [13]. The purification of the recombinant protein with glutathione-agarose (Sigma-Aldrich) was done as described in our previous report [14, 15]. The purity and integrity of the recombinant protein was confirmed by SDS-polyacrylamide gel electrophoresis. The protein was concentrated and separated from small peptide fragments, if any, with Centricon-10 (Millipore, Bedford, MA, http://www.millipore.com), and the solvent was changed from the elution buffer to the culture medium by dialysis.

Antigen Presentation Assay

A human CD4$^+$ T-cell clone, SA32.5, recognizing GAD65p111-131 in the context of HLA-DR53 molecule (DRA*0101+DRB4*0103) was established and maintained as previously described [16]. In the assay with the synthetic peptide, ES-DC stimulated with TNF-α (10 ng/ml) plus LPS (3 μg/ml) were harvested, incubated in the presence of peptide (6 μM) for 3 hours, washed four times with culture medium, and x-ray-irradiated (35 Gy). A T-cell proliferation assay was set up in a 96-well flat-bottomed culture plate with SA32.5 T cells (3×10^4 cells per well) and graded numbers of the peptide-loaded ES-DC in RPMI 1640 medium supplemented with 10% human plasma. In the assay with recombinant protein, the indicated amount of GST or GST-GAD protein was added to the coculture of SA32.5 T cells (3×10^4 cells per well) and irradiated ES-DC (1×10^4 cells per well). After 48 hours of culture, [^{3}H]-thymidine was added, and then after an additional 16 hours of culture, the cells were harvested and the incorporated radioactivity was counted.

Plasmid Construction

cDNA for human PD-L1 was isolated by polymerase chain reaction (PCR) with Pyrobest DNA polymerase (Takara, Osaka, Japan, http://www.takara.co.jp) using cDNA clone CS0DI011, purchased from Invitrogen (Carlsbad, CA, http://www.invitrogen.com), as a template. Double-stranded oligo DNA (5'-atgaacattttacttcagtatgtg-gtgaaaagtttcgat-3') coding for GAD65p115-127 (the core epitope for SA32.5 T-cell clone) was ligated to human invariant chain (Ii)-based epitope presentation vector pCI [17] to generate GAD65-epitope-fused Ii. A cDNA fragment for HLA-DRB4*0103 was generated by reverse transcriptase (RT)-PCR from RNA isolated from peripheral blood mononuclear cells positive for *HLA-DRB4*0103*. The coding DNA fragments were cloned into a mammalian expression vector, pCAG-IRES-Neo, which is driven by the CAG promoter and includes an internal ribosomal entry site (IRES)-neomycin-resistance gene cassette [3].

Transfection of ES Cells

Human ES cells were harvested using CTK solution, dissociated into clusters of 50-100 cells by pipetting, and washed twice with Dulbecco's modified Eagle's medium (DMEM). The cells harvested from two 90-mm culture dishes with subconfluently growing ES cells were suspended in 0.1 ml of DMEM and mixed with 50 μg of linearized plasmid DNA dissolved in 0.1 ml of PBS in a 4-mm-gap cuvette. The electroporation of human ES cells was performed at 150 V and 200 μF on a Gene Pulser (Bio-Rad, Hercules, CA, http://www.bio-rad.com). The transfection of cynomolgus monkey ES cells was done as previously described [18], with some modifications. Cynomolgus monkey ES cells were harvested after treatment with trypsin-EDTA. ES cells ($1-1.5 \times 10^7$) suspended in 0.7 ml of DMEM were mixed with 50 μg of plasmid DNA in 0.1 ml of PBS in a 4-mm-gap cuvette. Electroporation was done at 250 V and 500 μF. After electroporation, the ES cells were cultured on G418-resistant PEF feeder layers in 90-mm culture dishes or six-well plates. Selection with G418 (150 μg/ml) was done from 2 to 4 days after the transfection, and G418-resistant ES cell colonies were picked up using a micropipette under microscopic observation on days 15-18 for human ES cells and on day 11 for monkey ES cells. The transfectant clones were transferred to 24-well culture plates with PEF and expanded in the presence of G418. ES cell transfectant clones with relatively high levels of expression of the transgene were selected on the basis of the resistance to a high dose (1-3 mg/ml) of G418 and the results of the RT-PCR analysis. Thereafter, the clones were subjected to the differentiation procedures. At the proper stages of differentiation, the cells were screened to select ES cell clones that highly expressed the transgene after differentiation, based on a flow cytometric analysis for PD-L1 and Ii transfectant human ES cells and on the antigen-presenting capacity for HLA-DRB4 transfectant cynomolgus monkey ES cells.

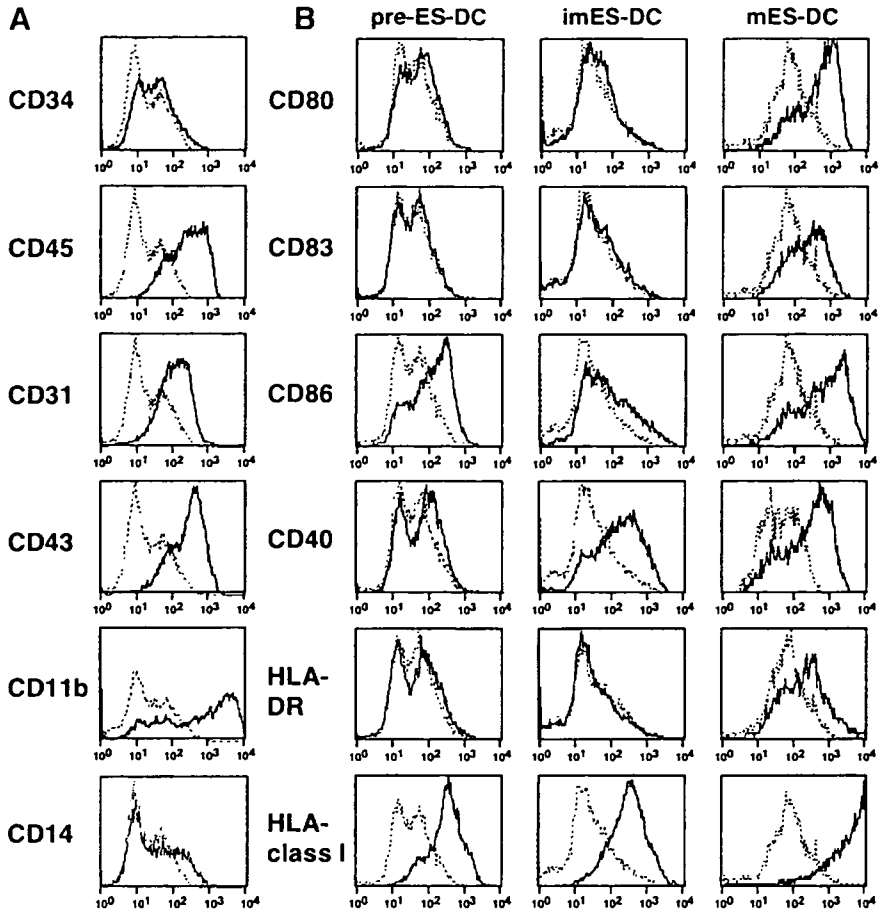

Figure 2. Cell surface phenotypes of human ES-DC. (A): ES cell-derived floating cells harvested on day 6 in the second step were analyzed for the cell surface expression of CD34, CD45, CD31, CD43, CD11b, and CD14. (B): ES cell-derived cells harvested on day 8 in the second step (pre-ES-DC) and from the third step before (imES-DC) and after (mES-DC) addition of maturation stimuli were analyzed for the cell surface expression of CD80, CD83, CD86, CD40, HLA-DR, and HLA class I. Staining profiles with specific antibody (Ab) (thick lines) and isotype-matched control Ab (thin, broken lines) are shown. Abbreviations: ES-DC, embryonic stem cell-derived dendritic cells; HLA, histocompatibility leukocyte antigen; imES-DC, immature embryonic stem cell-derived dendritic cells; mES-DC, mature embryonic stem cell-derived dendritic cells.

RT-PCR for Detection of the Transgene-Derived Transcripts

cDNA was synthesized from total cellular RNA with random hexamer primers and SuperScript II reverse transcriptase (Invitrogen). The following PCR primer sets were used: 5′-gctggattacatcaaagcactgaa-3′ and 5′-caacaaagtctggcttatatccaa-3′ for hypoxanthine-guanine phosphoribosyl transferase and 5′-ctgactgaccgcgttactcccaca-3′ and 5′-ttggttatagatgtatctgatcaggt-3′ for transgene-derived DRB4 transcript.

RESULTS

Differentiation of Human ES Cells to ES-DC

Based on previous experience in the generation of dendritic cells from mouse ES cells [1] and also based on the findings in a preliminary study using cynomolgus monkey ES cells, the feeder cell-coculture method was adopted for the generation of dendritic cells from human ES cells, instead of the embryoid body (EB)-based method. The human ES cell line selected was KhES-1; this line exhibited the highest growth rate among the three lines of human ES cell lines established in a recent study [9, 19]. For feeder cells, three lines of mouse stromal cell lines (ST2, OP9, and PA6) were evaluated for their capacity to induce hematopoietic differentiation of KhES-1 ES cells, and OP9 had the best yield among them (data not shown).

The protocol for the differentiation culture to generate ES-DC from human ES cells developed in the current study is composed of three steps, as shown in Figure 1A. At the beginning of the differentiation culture, undifferentiated ES cells maintained on mouse PEF feeders (Fig. 1B) were harvested using dissociation solution CTK [9] and plated on OP9 feeder cell layers (step 1). Next, the ES cells grew and formed clusters composed mostly of epithelial cell-like large flat cells (Fig. 1C, 1D). Clusters of round, cobblestone-like cells also appeared at approximately day 8, and those resembled the mesodermally differentiated cell clusters observed in hematopoietic differentiation culture of mouse ES cells [1, 20]. The size and number of round cell clusters gradually increased, and by around day 15, they covered 20%–30% of the surface area (Fig. 1E).

On days 15–18 of the first step, cells were recovered from the dishes using trypsin/EDTA and isolated nonadherent cells, and then they were seeded onto freshly prepared OP9 cell layers, to begin the second step. On the next day, the culture medium was exchanged for medium containing GM-CSF and M-CSF. Thereafter, small round cells, floating or loosely adhering to the feeder layer, appeared and gradually increased in number (Fig. 1F). The growth of the round cells depended primarily upon GM-CSF, thus suggesting that they grew in response to that factor. The cells were recovered and analyzed for their expression of hematopoietic cell lineage markers by flow cytometry (Fig. 2A). The cells expressed CD34 and CD45, thus indicating that they followed a hematopoietic cell lineage. They also expressed CD31, CD43, and CD11b, thus collectively indicating a commitment to a myeloid cell lineage. The double peaks seen in the histograms in Figure 2 reflect the heterogeneity of the analyzed cells in size and intensity of autofluorescence.

On days 7–10 of the second step, the floating or loosely adherent cells were harvested by pipetting and transferred to Petri dishes without feeder cells. We then cultured the cells in the presence of GM-CSF and IL-4 to start the third step. Following this passage, the cells changed their morphology from round to irregular shapes, and some had protrusions (Fig. 1G).

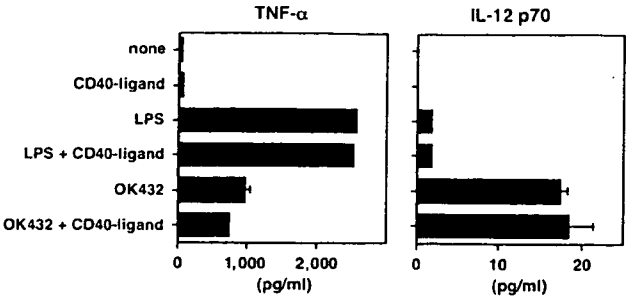

Figure 3. Production of TNF-α and IL-12 by embryonic stem cell-derived dendritic cells (ES-DC). ES-DC were recovered from the culture (third step, day 4) and replated (1.2×10^5 cells per 150 μl in 96-well culture plates) in the presence or absence of soluble CD40-ligand (20 ng/ml), LPS (3 μg/ml), or OK432 (10 μg/ml) as indicated. After 60 hours, supernatant was collected, and concentration of TNF-α and IL-12 p70 was measured by enzyme-linked immunosorbent assay. Data are indicated by mean value + SD of duplicate cultures. Abbreviations: IL, interleukin; LPS, lipopolysaccharide; TNF-α, tumor necrosis factor α.

Cells with protrusions gradually increased, and more than 50% of the cells exhibited DC-like irregular shapes after 2–3 days (Fig. 1H). The floating cells expressed CD86 and CD40 but scarcely expressed CD80 or CD83 (Fig. 2B). Expression of HLA-DR at this stage differed between experiments.

Figure 1I and 1J shows the cells after the simultaneous addition of TNF-α, LPS, soluble CD40-ligand, and IL-4. Generally, they exhibited longer protrusions than before the stimulation, and some of the protrusions were veil-like. Many of the cells formed aggregates. Flow cytometric analysis showed the increased expression of CD86 and the expression of CD80, CD83, and HLA-DR (Fig. 2B). Collectively, the cells exhibited the characteristics of DC in their morphology and expression of surface molecules, and thus they were designated human ES-DC.

Production of IL-12 and TNF-α by ES-DC was measured by ELISA (Fig. 3). Production of TNF-α was profoundly induced by either LPS or OK432. OK432, but not LPS, induced the production of IL-12, consistent with the reports that OK432 is an efficient inducer of IL-12 [21, 22]. Addition of CD40-ligand showed little effect on the production of these cytokines by human ES-DC.

ES cell-derived floating cells first appeared during the second step of the culture for differentiation (pre-ES-DC) and could readily be isolated by the pipetting procedure. Their morphology, pattern of expression of surface molecules, and T-cell-stimulation capacity (described below) continuously changed until the final maturation. To determine the change in gene expression associated with such changes in the phenotypes, the gene expression profiles of pre-ES-DC, immature ES-DC, and mature ES-DC were analyzed using cDNA microarrays. For reference purposes, human peripheral blood monocytes and immature and mature Mo-DC were also analyzed. The data for genes with relevance to immune functions were selected from the total microarray data and are shown in supplemental online Table 1. Consistent with the results of flow cytometric analysis (Fig. 2B), upregulation of the expression of genes encoding cell surface molecules such as HLA class I, HLA class II, CD86, and CD40, along with differentiation of ES-DC, was observed. In addition, expression of the genes related to DC function, including CD74/invariant chain, CCR7, and CCL17/TARC, was increased during the differentiation. Clustering analysis indicates similarity between change of the gene expression pattern from monocytes to immature Mo-DC and that from pre-ES-DC to immature ES-DC, as well as that from immature Mo-DC to mature Mo-DC and that from immature ES-DC to mature ES-DC (supplemental online Fig. 1).

The protocol of differentiation culture described thus far was originally developed using the KhES-1 line of human ES cells. This differentiation procedure was also applied to KhES-3, another human ES cell line. KhES-3 differentiation was similar to KhES-1 except that KhES-3 differentiated slightly more quickly than KhES-1, and a first-step culture of 14–15 days was sufficient for the differentiation of KhES-3.

Function of Human ES-DC

The capacity of the human ES-DC to stimulate T cells was examined based on the proliferative response of allogeneic T cells cocultured with ES-DC (Fig. 4A). ES cell-derived floating cells recovered from the second step (pre-ES-DC) showed little capacity to induce a response of T cells. In contrast, ES-DC following the third step before the addition of maturation stimuli (immature ES-DC) showed a weak but definite stimulation, and following exposure to the maturation stimuli (mature ES-DC) they showed a strong capacity to stimulate allogeneic T cells to proliferate.

Next, the antigen-presenting capacity of ES-DC was examined. KhES-1 is positive for the *HLA-DRB4*0103* gene encoding the β chain of HLA-DR53 molecule. Presumably, ES-DC derived from KhES-1 should express the DR53 molecule, and their ability to present antigen to DR53-restricted $CD4^+$ T cells was determined. As shown in Figure 4B, KhES-1-derived ES-DC preloaded with GAD65-derived synthetic peptide stimulated GAD65-specific DR53-restricted human T-cell clone SA32.5 to proliferate. To examine the capacity to process antigenic protein and present epitope, recombinant protein was used as the antigen (Fig. 4C). The SA32.5 T-cell clone cocultured with the ES-DC in the presence of recombinant GAD65 protein also showed a proliferative response, thus indicating that ES-DC processed the antigenic protein and presented the epitope derived from the protein in the context of HLA class II molecules.

Genetic Modification of Human ES-DC

Previous research established a strategy for the genetic modification of mouse ES-DC [1]. Briefly, the expression vectors were introduced into ES cells by electroporation, and subsequently the transfectant ES cell clones were induced to differentiate to ES-DC. The following experiments were performed to determine whether or not this strategy could be applicable to human ES cells.

PD-L1/B7-H1 is known to downmodulate responses of T cells upon interaction with the ligand, PD-1 on T cells [23]. An expression vector for human PD-L1 was introduced to KhES-1 by electroporation. The expression vector used was pCAG-INeo, driven by the CAG promoter and containing an IRES-neomycin-resistance gene cassette (Fig. 5A). Among the transfectant clones, 23 ES cell clones showing resistance to high does of G418 (2 mg/ml) were selected and subjected to the ES-DC-differentiation culture.

The expression of PD-L1 of the transfectant clones was examined by a flow cytometric analysis at the stage of immature ES-DC, harvested on day 2 of the third step of the differentiation culture. Although even nontransfectant ES-DC evidently expressed PD-L1 after maturation (data not shown), only a small population of them expressed PD-L1 at this stage (Fig. 5B, K1ES-DC). On the basis of the results of the analysis, one transfectant clone, KhES1-PD28, expressing the highest level of PD-L1 after the differentiation into immature ES-DC, was selected (Fig. 5B). Allogeneic T cells cocultured with immature ES-DC-PD28 showed a significantly lower response than those cocultured with nontransfectant immature ES-DC ($p < .05$; Fig.

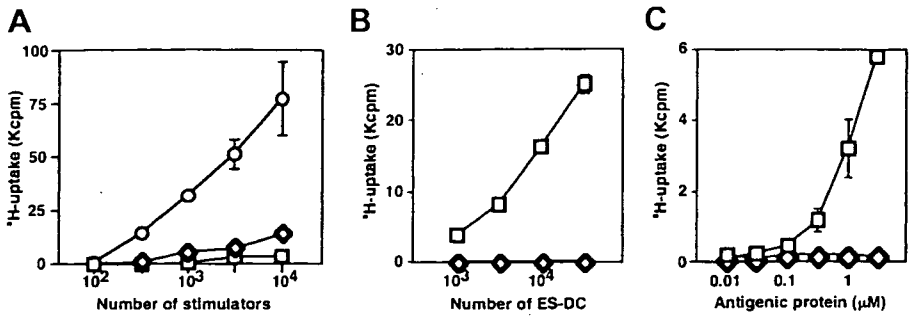

Figure 4. Stimulation of allogeneic T cells and antigen presentation by human ES-DC. **(A):** The indicated numbers of mature ES-DC (circles), immature ES-DC (diamonds), and pre-ES-DC (squares) were x-ray-irradiated (40 Gy) and cocultured with allogeneic human peripheral blood T cells (4×10^4 cells per well) in a 96-well round-bottomed culture plate for 5 days. Proliferation of T cells in the last 16 hours of the culture was measured based on [^{3}H]-thymidine uptake. The data are indicated as the mean value ± SD of duplicate cultures. **(B):** The indicated numbers of KhES-1-derived mature ES-DC prepulsed with glutamic acid decarboxylase (GAD) $65_{111-131}$ peptide (squares) and those left unpulsed (diamonds) were cocultured with a GAD65-specific, HLA-DR53-restricted human CD4$^+$ T-cell clone, SA32.5 (3×10^4 T cells per well) for 3 days. Proliferation of the T cells in the last 16 hours of the culture was measured by [^{3}H]-thymidine uptake. **(C):** Mature KhES-1-derived ES-DC (1×10^4 cells per well) were cocultured with SA32.5 T cells (3×10^4 cells per well) in the presence of the indicated concentrations of glutathione *S*-transferase (GST)-GAD65 recombinant protein (squares) or GST protein (diamonds) for 3 days. Proliferation of the T cells in the last 16 hours of the culture was measured by [^{3}H]-thymidine uptake. Abbreviation: ES-DC, embryonic stem cell-derived dendritic cells.

5C). The proliferation-reducing effect of the transgene-derived PD-L1 was abrogated by the addition of anti-PD-L1 blocking Ab ($p < .01$), ruling out the possibility that the introduction of the PD-L1 expression vector impaired the differentiation of ES-DC. Collectively, these results suggest that forced expression of PD-L1 on ES-DC downmodulated the proliferative response of cocultured allogeneic T cells via the interaction of PD-L1 with PD-1 on the T cells.

ES-DC carrying an epitope-presenting vector and expressing recombinant human invariant chain (Ii/CD74), which included GAD65p115–127 in the class II-associated invariant chain peptide region, were also generated (Fig. 5D). It was expected that the epitope could be efficiently targeted to the major histocompatibility complex (MHC) class II pathway [17]. Using a protocol similar to that used for the generation of PD-L1 transfectants, the vector was introduced into KhES-1 ES cells, and a transfectant clone, KhES-1-Ii23, highly expressing transgene-derived recombinant CD74, was selected by a flow cytometric analysis at the pre-ES-DC stage. The expression of CD74 was detected even in the nontransfectant pre-ES-DC, reflecting intrinsic expression of CD74 (Fig. 5E). The transfectant exhibited an increased expression of CD74 in comparison to the nontransfectants, thus indicating additional expression of the molecule derived from the transgene. The ability of the transfectant ES-DC, ES-DC-Ii23, to stimulate the GAD epitope-specific T-cell clone SA32.5 in the absence of antigenic peptide or protein was next examined. As a result, ES-DC-Ii23 stimulated SA32.5 T cells and induced their proliferation, thus demonstrating functional expression of the epitope-presentation vector in the transfectant ES-DC (Fig. 5F). The in vivo transfer of ES-DC transfected with this antigen-presenting vector is therefore expected to be useful for controlling the immune response in an antigen-specific manner [7].

Generation and Genetic Modification of Cynomolgus Monkey ES-DC

The differentiation protocol established using human ES cells was then applied to nonhuman primate ES cells. An ES cell line derived from cynomolgus monkey, CMK6 [11], was subjected to the ES-DC differentiation culture. Following the transfer to OP9 feeder layers, CMK6 cells grew and differentiated more rapidly than did human ES cells KhES-1 and KhES-3. The optimal duration of the first step of the differentiation culture for CMK6 was 11–13 days, whereas the duration ranged from 14 to 18 days for human ES cells. Figure 6A–6C illustrates the morphological changes of CMK6-derived cells following the second step of the differentiation culture. The surface phenotypes of the CMK6-derived pre-ES-DC, immature ES-DC, and mature ES-DC were then analyzed by flow cytometry (Fig. 6D). The double peaks seen in the histograms in Figure 6D reflect the heterogeneity of the analyzed cells in size and intensity of autofluorescence. Cynomolgus monkey ES-DC had the capacity to stimulate allogeneic cynomolgus monkey T cells (Fig. 6E), as human ES-DC did.

The expression vector for *HLA-DRB4*0103* (Fig. 7A) was introduced to CMK6. An analysis of the partial nucleotide sequence of *DRA* (*CyLA-DRA*) gene of CMK6 showed that the predicted amino acid sequence of the CyLA-DRα chain is very similar to that of HLA-DRα, with only one amino acid difference in α1 domain (GenBank accession no. AY591919). This suggested that the transgene-derived HLA-DRβ chain could associate with the intrinsic CyLA-DRα chain expressed in cynomolgus ES-DC and present an antigen to human T cells. The expression of the transgene before and after the ES-DC differentiation was confirmed by an RT-PCR analysis (Fig. 7B). ES-DC derived from a transfectant ES cell clone, cES-53-23, were prepulsed with synthetic GAD65 peptide and cocultured with the HLA-DR53-restricted, GAD65-specific T-cell clone SA32.5. Figure 7C shows that the GAD65 peptide-pulsed transfectant ES-DC stimulated the T cells to proliferate. In contrast, ES-DC originating from parental ES cells prepulsed with the peptide could not stimulate the T-cell clone. In addition, DR53-transfectant cynomolgus ES-DC had the capacity to process and present a protein antigen to the T cells (Fig. 7D). These results demonstrate the antigen-processing and presenting capacity of cynomolgus ES-DC and also the functional expression of the transgene that had been introduced into the ES cells before the differentiation. Thus, the effect and safety of the immune therapy by the in vivo transfer of ES-DC can be examined by preclinical studies using cynomolgus monkeys.

DISCUSSION

To establish the current culture protocol, various culture conditions were tested. As feeder cell lines, three lines of mouse stromal cells, OP9, PA6, and ST2, were comparatively evaluated. As a result, the use of OP9 was thus observed to produce

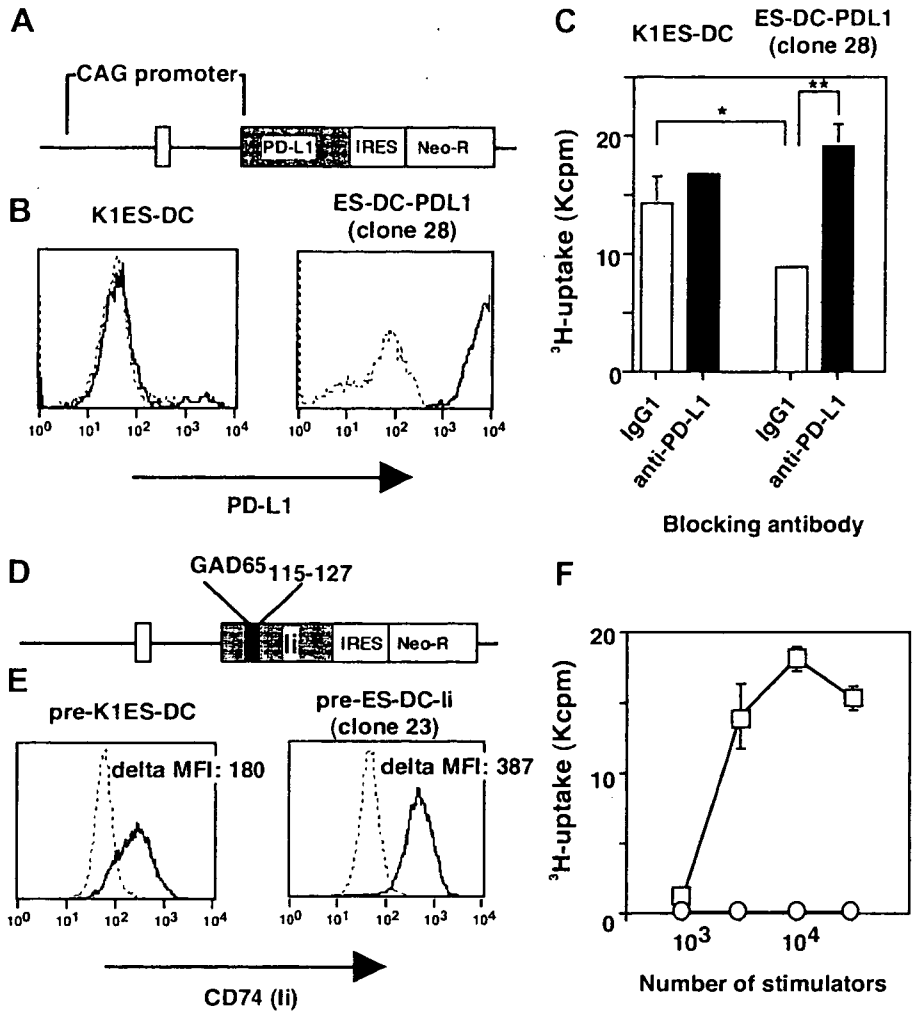

Figure 5. Genetic modification of human ES-DC. **(A):** Structure of the expression vector for human PD-L1. The expression of PD-L1 was driven by the CAG promoter, and the PD-L1-coding sequence was followed by IRES-neomycin-resistance gene (Neo-R), a selection marker. The open box in the CAG promoter indicates exon 1 of the rabbit β-actin gene contained in CAG promoter. **(B):** Transgene-derived PD-L1 expressed in immature ES-DC originated from transfectant embryonic stem (ES) cells was detected by flow cytometric analysis (ES-DC-PD-L1, clone 28). As a control, the staining profile of ES-DC derived from parental ES cell line (K1ES-DC) is shown. Specific stainings with anti-human-PD-L1 monoclonal antibody (Ab) (thick line) and isotype-matched control staining (thin, broken line) are shown. **(C):** The alloreactive response of T cells (4×10^4 cells per well) cocultured with immature ES-DC (1×10^4 cells per well) derived from the PD-L1-transfectant ES cells (ES-DC-PD-L1, clone 28) or those derived from parental ES cell line (K1ES-DC) is shown. The culture was done under the same conditions as those shown in Figure 3A except that anti-PD-L1 blocking Ab or isotype-matched mouse IgG1 was added to the culture. The statistical significance of the differences between the T-cell responses is indicated by asterisks (*, $p < .05$; **, $p < .01$). **(D):** Structure of expression vector for human Ii (Ii/CD74) including GAD65-derived epitope. The class II-associated invariant chain peptide region of the Ii-coding sequence was replaced with an oligo DNA-encoding $GAD65_{115-127}$. **(E):** Intracellular CD74 expressed in pre-ES-DC originated from transfectant ES cell clone (pre-ES-DC-human Ii [hIi], clone 23) and parental ES cell line (pre-K1ES-DC) was detected by a flow cytometric analysis. Specific staining with anti-human-CD74 monoclonal Ab (thick lines) and isotype-matched control staining (thin, broken lines) are shown. The values in the figure indicate the delta MFI between staining with the anti-CD74 and the isotype-matched control Ab. **(F):** SA32.5 T cells (3×10^4 cells per well) were cocultured with the indicated numbers of mature ES-DC-hIi clone 23 (squares) or nontransfectant ES-DC (circles) in the absence of exogenous antigen for 3 days. The proliferation of the T cells in the last 16 hours of the culture was measured by the [^{3}H]-thymidine uptake. Abbreviations: delta MFI, difference of mean fluorescence intensity; ES-DC, embryonic stem cell-derived dendritic cells; GAD, glutamic acid decarboxylase; Ii, invariant chain; IRES, internal ribosomal entry site.

the highest yield of ES-DC. Although ST2 also worked as feeder cells in the second step, the yield of ES-DC was approximately half of that obtained using OP9. It was also essential to remove any firmly adherent cells, when transferring the cells from the first to second step, by the procedure described in the Materials and Methods. At the end of the first step, many flat, adherent ES cell-derived cells were observed to form monolayers in the dishes. They probably differentiated into cell lineages other than mesoderm, and unless removed, they grew rapidly in the second step and inhibited the growth of hematopoietic cells.

Previously, two other groups reported the generation of functional antigen-presenting cells or DC from human ES cells. Zhan et al. adapted embryoid body-based induction of hematopoietic differentiation [24]. Slukvin et al. recently reported a method using OP9 [25]. Although there are some similarities between the method of Slukvin et al. [25] and the one reported here, the two methods differ in the following points.

In both methods, human ES cells were cocultured with OP9 feeder cells at the initial differentiation step (the first step). However, the duration of this culture step in our method (14–18 days) is significantly longer than the 10 days in the method of Slukvin et al. [25]. In our system, cells with morphology indicating mesodermal differentiation first appeared on day 8 or 9, and the extension of the first step of culture to days 14–18 significantly improved the yield of hematopoietically differentiated cells (Fig. 1D, 1E). In addition, we pretreated OP9 cells